The role of convection in winter mixed layer formation in the Gulf of Maine: February 1987

Prashant Mupparapu and Wendell S. Brown

Ocean Process Analysis Laboratory, Institute for the Study of Earth, Oceans, and Space, Department of Earth Sciences, University of New Hampshire, Durham, New Hampshire. Submitted to *J. Geophys. Res./Oceans*, 29 October 1999.

Abstract. Moored hourly observations of temperature and salinity from the Wilkinson Basin in the western the Gulf of Maine, augmented with gulf-wide hydrography survey, document the winter mixed layer evolution between 4 and 18 February 1987. Wind stresses and air-sea heat fluxes were estimated from the Gulf of Maine (44005) National Data Buoy Center buoy winds and temperatures using bulk formulae. During the study period, a pair of strong cooling episodes due to offshore (southeastward) winds bracketed an even stronger cooling event due to a strong northeasterly storm. The 0-165 m water column cooled during the study period. Heat budgets based on the observations show that local air-sea heat loss could only explain cooling in the upper 35-60 m of the Wilkinson water column. Lateral advection must have caused the deeper cooling. The one-dimensional bulk mixed layer model of Price, Weller, and Pinkel [*Price et al.*, 1986], forced with observed surface fluxes, exhibited a mixed layer that deepened from about 60 m to 120 m during initial stages of the nor'easter in general accordance with observation. Diagnostic PWP model experiments showed that convective overturning was required to produce the observed mixed layer depth of 120 m. Conversely, direct wind mixing alone could deepen the model mixed layer to only about 80 m. However, the model property profiles produced by a ten-day PWP model run differed significantly from observations, which reflected advection effects. Observed hydrographic property distributions combined with horizontal velocity estimates from a Dartmouth linear 3-D, finite element circulation model of the Gulf (FUNDY5) help to explain differences between the PWP model and observations in terms of lateral advection in the upper 65 m. The observed cooling between 65 m and 165 m must be related to advection.

Introduction

Winters in many high latitude marginal sea regions are marked by frequent episodes of cold, dry offshore winds. In such regions, usually to the south and east of continental land masses, episodic winds cool the surface waters of the ocean rapidly, increasing their density relative to that of the waters below [*Stommel*, 1972]. This unstable situation sets the stage for convection to augment wind mixing in the deep vertical mixing of the upper water column. The intensity of these processes determines the ultimate depth of winter mixed layer and the amount of the winter water mass, which is formed in the process.

Many similar aspects of the convective-overturning process have been observed in different marginal seas, including the Gulf of Lions in the western Mediterranean Sea [*Stommel*, 1972; *Schott and Leaman*, 1991], the Greenland Sea [*Schott et al*., 1993] and the Labrador Sea [*Clarke and Gascard*, 1983]. Oceanic sites exhibiting deep convective mixing are generally associated with cool, fresh water overlying warmer, saltier water and a basin-scale cyclonic gyre. *Stommel*

[1972] suggested that such sites are especially susceptible to preconditioning by the combined effect of mechanical wind mixing and atmospheric cooling to erode the stratification by convection during autumn. In noting these and other similarities, *Killworth* [1983] describes the process of winter water production in terms of this surface water preconditioning, followed by episodic "violent" mixing/sinking which produces new winter water. In the latter phase the newly formed dense winter water equilibrates with the surrounding water and in a slower, more diffusive process, spreads to form the precursor to an intermediate or deep water mass.

The winter convection-induced water formation process described above is organized on a hierarchy of scales. The surface convective (i.e., density-induced) plumes, which represent one of the smaller convection scales, have lateral scales of the same order as the mixed layer depth, which can range from 10 m to 1000 m depending upon location [*Gascard*, 1991]. The corresponding formation time scales of these convective plumes range from hours to a day. The water masses produced by the convective plumes fill "chimney-scale" (~50 km) zones of nearly homogeneous water. *Gascard* [1991] reports finding mesoscale (1-10 km) eddies around the edge of the "chimneys." Thus it appears that the plumes and eddies combine to homogenize the water column and form these chimney-scale zones of winter water.

Many conditions in the Gulf of Maine (Figure 1), including its location downwind of arctic air masses and a distinct intermediate water mass, mimic those of the deeper marginal sea oceanic regions. *Hopkins and Garfield* [1979] and *Brown and Irish* [1993] have described the seasonally varying three-layer water mass system of the Gulf of Maine. Maine Surface Water (MSW) characteristics are strongly influenced by the seasonal changes in the surface heat transfer processes, local runoff and an influx of cold, fresh Scotian Shelf Water (SSW). The deeper Maine Bottom Water (MBW) is derived from mixtures of warm, salty continental slope water (SW) through the Northeast Channel and the Maine Intermediate Water (MIW). The latter is characterized by its minimum temperature is a remnant of a cold, mixed layer water produced primarily during the previous winter. Solar warming during the spring separates the winter water into MSW and MIW. *Brown and Irish* [1993] found that, while varying annually, the thickest MIW layer was found in the Wilkinson Basin part of the Gulf of Maine throughout the year.

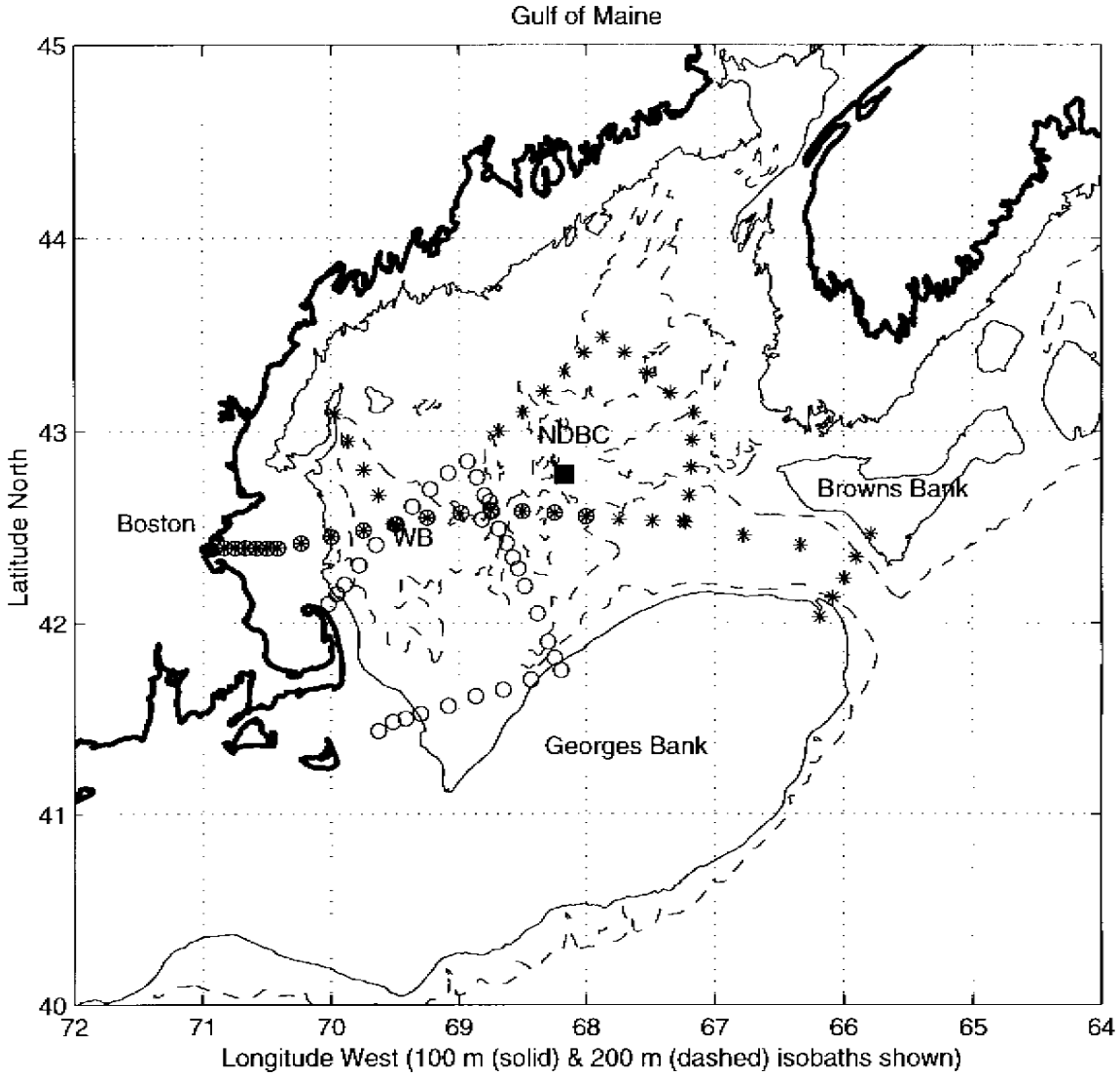

Figure 1. A Gulf of Maine location map showing R/V Oceanus February 1987 *hydrographic survey* stations for 5-8 (open dots), 10-15 (asterisks), and 15-20 (+). The Wilkinson Basin *T/C mooring* site (WB) and the NDBC *meteorological buoy* (square) are also located.

It would appear that the Wilkinson Basin proximity to the southwestern coast of the Gulf and the observed tendency for cyclonic flow in the winter [*Vermersch et al.*, 1979] are factors in the predominance and persistence of Wilkinson Basin MIW. *Brown and Irish* [1993] attribute the cyclonic flow tendency to a pulse of dense MBW and Slope Water, which they "tracked" from the Northeast Channel in early summer to Wilkinson Basin by late summer 1987. This annually reoccurring process in part explains the cyclonic flow and the corresponding isopycnal doming observed in the Wilkinson Basin by *Brown and Irish* [1993] in February 1997. Thus the preconditioning of the Wilkinson Basin for subsequent winter convective mixing appears to be part of the annual hydrographic cycle in the Gulf.

Cold offshore winds also occur predictably each winter in the Gulf of Maine. *Bunker* [1956] describes an early winter process whereby these cold offshore winds preferentially extract heat from the shallower coastal waters of the Gulf. The Figure 2 SST image illustrates this across the isobath (downwind) temperature gradient during winter 1995. As the offshore flowing air is cooled, the sea-air heat transfer tends to decrease offshore. *Brown and Beardsley* [1978] linked measured unstable density profiles in the coastal western Gulf of Maine during the winter of 1974-75 to full water column (~150 m) convective mixing. The *Brown and Irish* [1993] moored observations of intermittent instability of the water column in Wilkinson Basin in early February 1987 are evidence that convection-induced water column mixing (to depths of about 150 m) is also important there. Thus the Gulf of Maine appears to be a useful site for studying globally important convection-induced water mass formation processes.

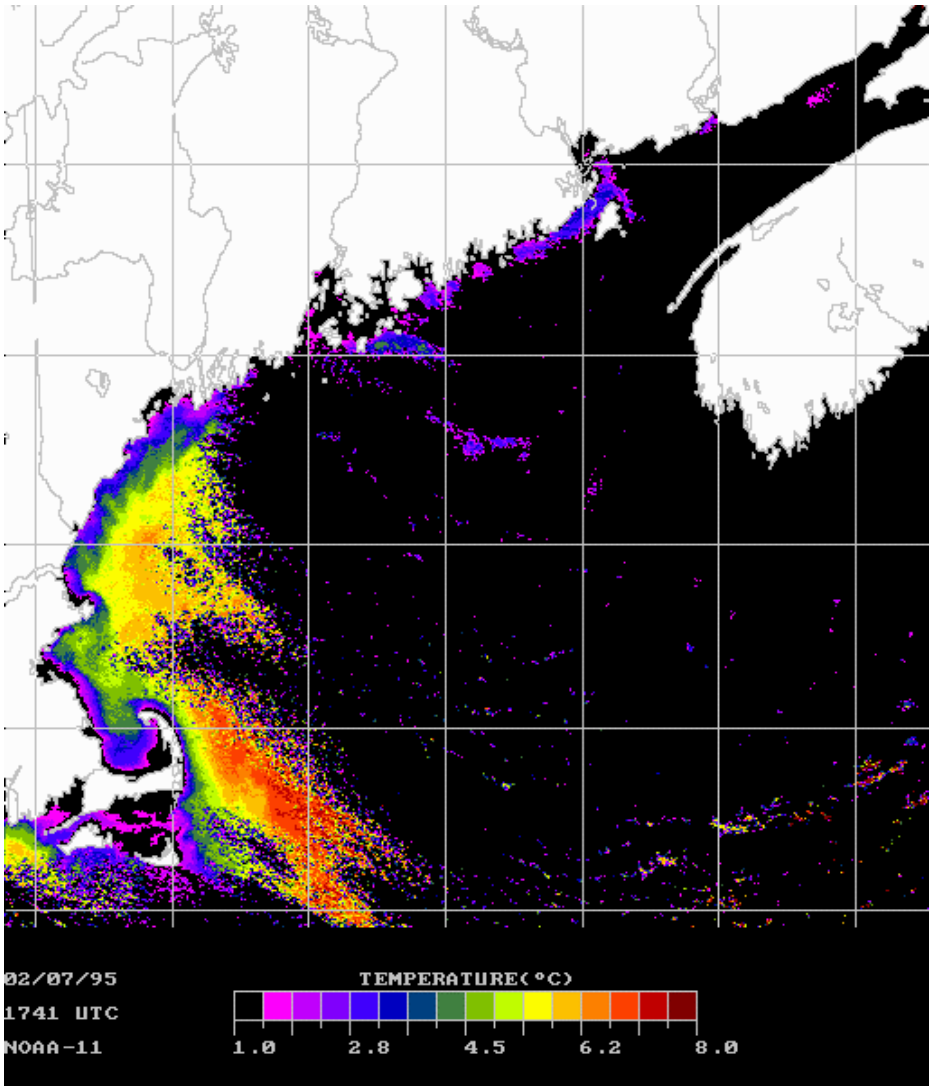

Figure 2. A NOAA-11 sea surface temperature (SST) image of the Gulf of Maine on 7 February 1995 at 1741 (UTC) clearly shows the coldest SSTs along the coast in the western Gulf—undoubtedly due to strong heat extraction by the cold westerly winds. The offshore cloudiness, also typical for these conditions, is likely related to the intense air-sea interaction. Note the "warmer" water around the unobscured edges of Wilkinson Basin.

This paper describes an in-depth analysis of the February 1987 *Brown and Irish* [1993] observations in terms of convection-induced mixing and winter water mass formation in the western Gulf of Maine. In section 2, moored buoy data, wind observations and estimates of air-sea heat and momentum fluxes for 4-18 February 1987 are described. In section 3, the use of a one-dimensional mixed layer model to assess the relative importance of convective and wind mixing in the water mass formation process is described. In section 4, advective effects on the water formation process are evaluated with the help a three-dimensional circulation model. In section 5, we discuss the implications of the modeling results and summarize.

Description of Data Set

The meteorological forcing in Wilkinson Basin has been estimated using meteorological records from the nearby Gulf of Maine National Data Buoy Center buoy (NDBC 44005; see Figure 1 for location). The hourly buoy winds were used to estimate wind stresses with the *Large and Pond* [1981] bulk formula

$$\vartheta = \Delta_a \, C_D \, U \, \mathbf{U} \, ,$$

where Δ_a = 1.22 kg m^{-3} is the nominal density of air, **U** is the vector wind (adjusted to an elevation of 10 m) and C_D is the wind speed-dependent neutral stability drag coefficient (ranging from 1.3-1.6 x 10^{-3}). The strongest wind stresses exceeded 0.8 Pascals (or Nm^{-2}), early on 10 February (Figure 3).

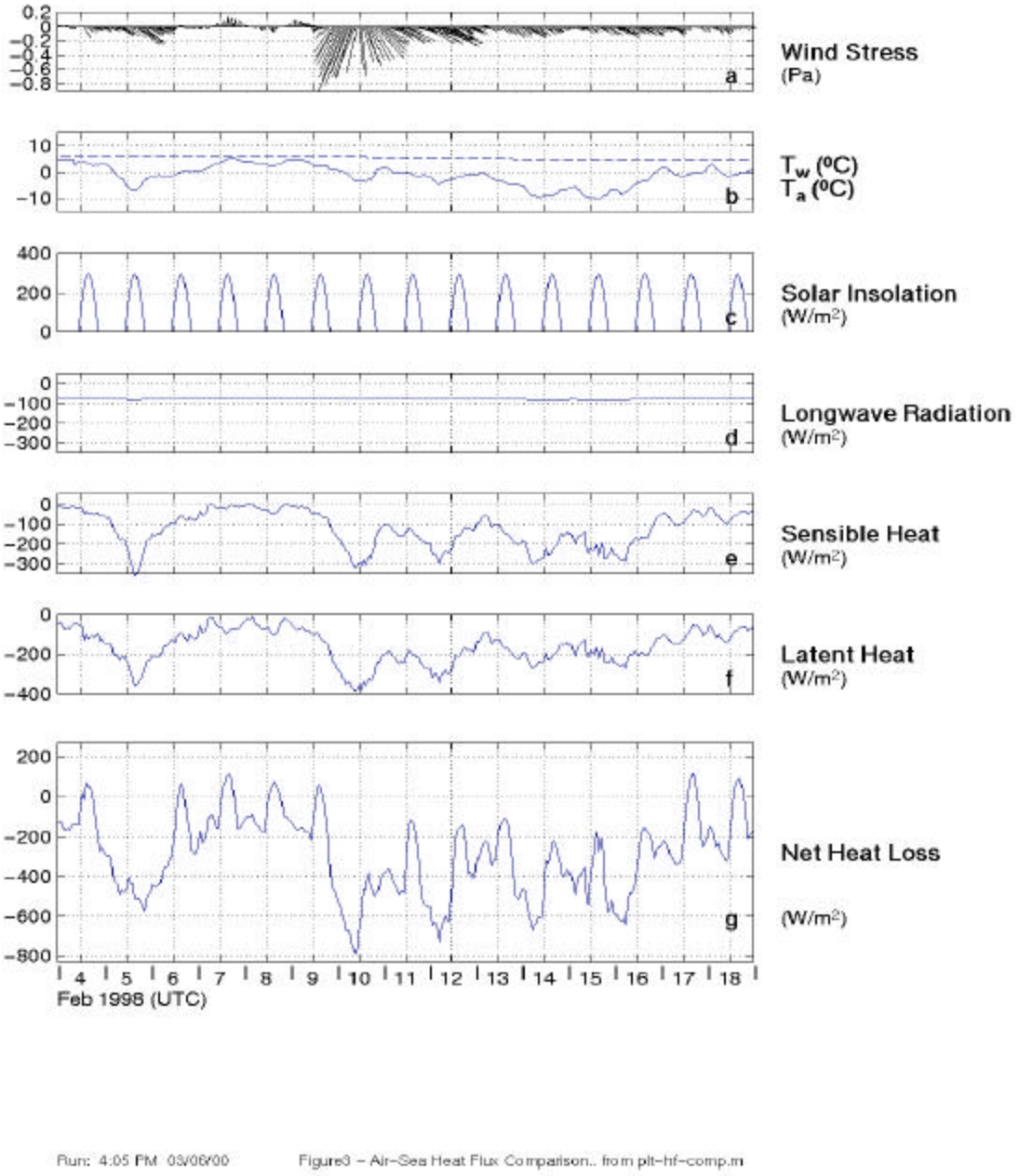

Figure 3. Time series of wind stress and thermodynamic surface forcing from 4 to 18 February 1987. Panel (a) shows a sequence of hourly wind stress vectors derived from winds on the NDBC buoy near Wilkinson Basin in the central Gulf. Panel (b) shows the air and ocean temperatures in Wilkinson Basin. Estimates (see text) of the components of the panel (g) net heat flux to the ocean surface are shown in the intervening panels.

The total local air-sea heat flux record for this time period was determined by summing estimates of incoming solar insolation, and heat losses due to the latent, sensible, and long-wave radiative heat fluxes. The bulk air-sea heat flux algorithms used for these heat flux estimates are presented in Appendix A. While we had time series measurements from which to compute many of the heat flux components, estimating solar insolation and latent heat flux posed problems. Without detailed observations of cloudiness at the Wilkinson Basin site, we improvised. First we assumed a standard half-sinusoidal form for clear sky solar insolation for the whole study period (Figure 3). The amplitude of this clear-sky insolation was corrected for the climatological average cloudiness in the Gulf of Maine for the month of February. Therefore, while the day-to-day details are inaccurate, the total incoming solar radiation heat was climatologically correct and probably reasonable for the study period. We also benefit from the fact that February latent and sensible heat flux losses together are much greater than the solar insolation.

Estimates of the sensible and latent heat fluxes, using the *Beardsley et al.* [1998] modified versions of the TOGA-COARE formulae [*Fairall et al*., 1996], suggest that our heat loss estimates may be too large by about 30%. However, given the general uncertainty in which algorithms are best suited for these particular circumstances, we present both estimates as a measure of the uncertainty in the actual heat flux forcing. We later explore the impact of this uncertainty on the results.

Despite the uncertainty in the actual values of the heat flux forcing we are confident in the principal features of the net air-sea heat flux record which consisted of (1) a 5-6 February cooling period due to strong air-sea temperature difference and moderate winds; (2) a couple days of near-zero net heat loss (daily solar warming was approximately offset by nightly cooling); (3) a 9-13 February storm-induced cooling period due to strong winds and moderate temperature differences; concluded by (4) a 14-17 February cooling period due to large temperature differences and moderate to weak winds. Thus, during the fourteen-day study period, there were two different kinds of atmosphere-ocean heat and momentum exchange scenarios, which produced similarly intense heat extraction.

The ocean response to the heat flux and wind stress forcing is derived from shipboard hydrography and moored hourly observations of water properties in Wilkinson Basin (WB) from the *Brown and Irish* [1993] field study conducted between August 1986 and September 1987. The gulfwide shipboard hydrography survey, which began on 5 February, was interrupted by the storm for most of 9-10 February, before resuming on 11 February. To extend the spatial coverage we also include the 16-20 February measurements kindly provided by D. Townsend. Representative CTD sigma-theta profiles from 8 February before and 15 February after the storm (Figure 4) show (a) that the surface mixed layer shallowed from about 120 m before the storm to about 60 m after the storm, and (b) a deeper mixed layer between 100 and 150 m. As indicated by the corresponding T-S diagrams, the upper layer freshening was primarily responsible for the principal structural changes. A comparison of the water properties—derived from CTD and moored temperature and conductivity measurements (Figure 4)—shows that the moored measurements resolve the main structural features of the water column.

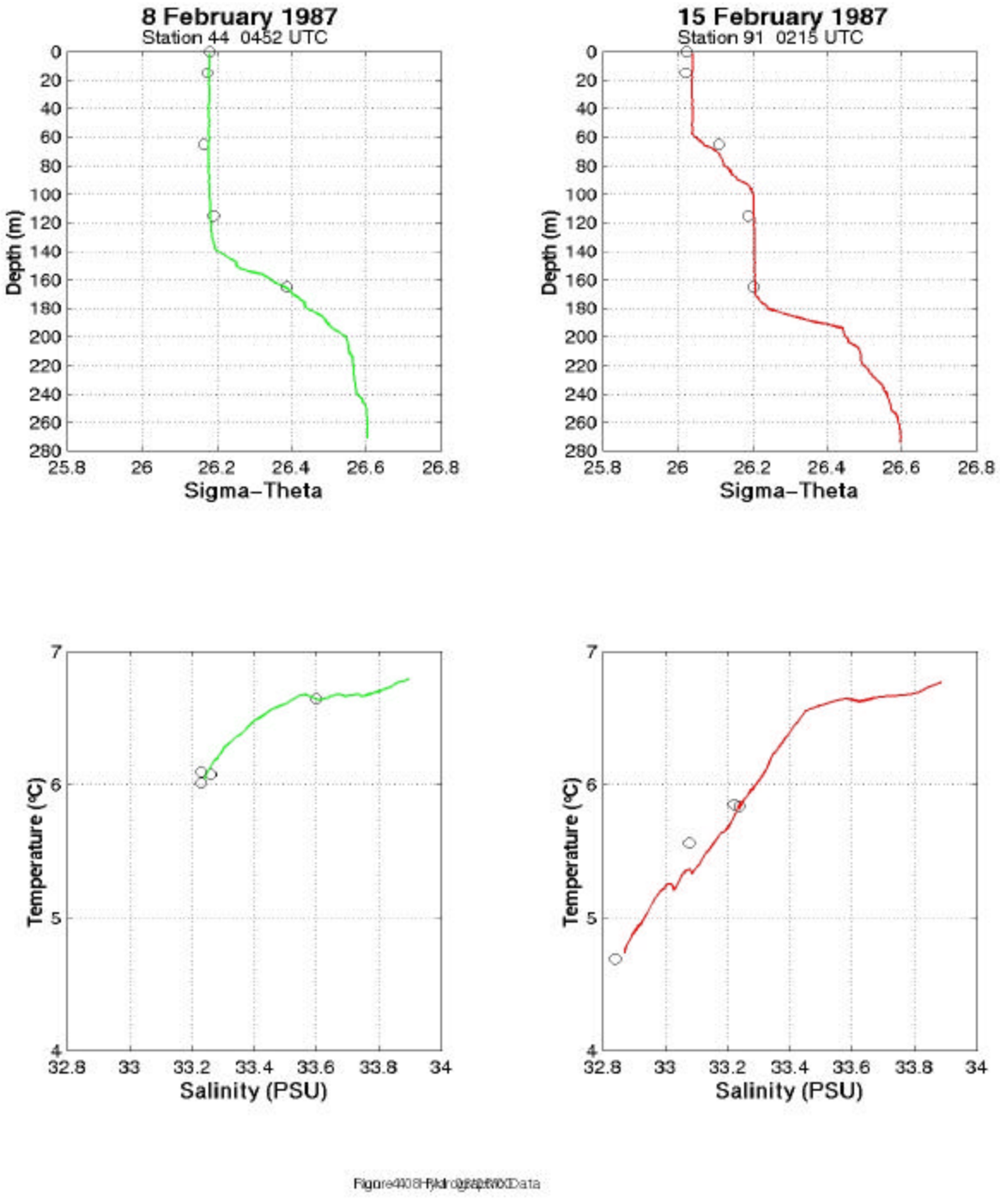

Figure 4. Sigma-theta profiles next to the Wilkinson Basin mooring site before and after the 9-10 February storm. The sigma-theta values derived from the nearest hourly-averaged temperature and conductivity measurements on the mooring are shown for comparison. The corresponding potential temperature versus salinity relations show the storm-related freshening (and cooling) of the upper 165 m.

As revealed in the salinity sections before the 9 February 1987 storm (Figure 5), the upper 115 m of the central Wilkinson Basin water column was a relatively fresher (and colder) homogeneous layer on top of saltier, warmer deeper water. Except near the surface, the basic water density distribution by salt distribution is dictated. A comparison of the across-gulf salinity sections from before and after the storm strongly suggests that there was advection of fresher (i.e., less dense, though colder) upper water into the region of the Wilkinson Basin T/S mooring during and after the storm. The surface temperature and salinity maps (Figure 6) indicate a northern coastal source region for the fresher (and cooler) water. The stratifying effects of the fresher water mass appear to have been responsible for the shallower surface mixed layer that was observed after the storm, as shown by the moored T-S measurements.

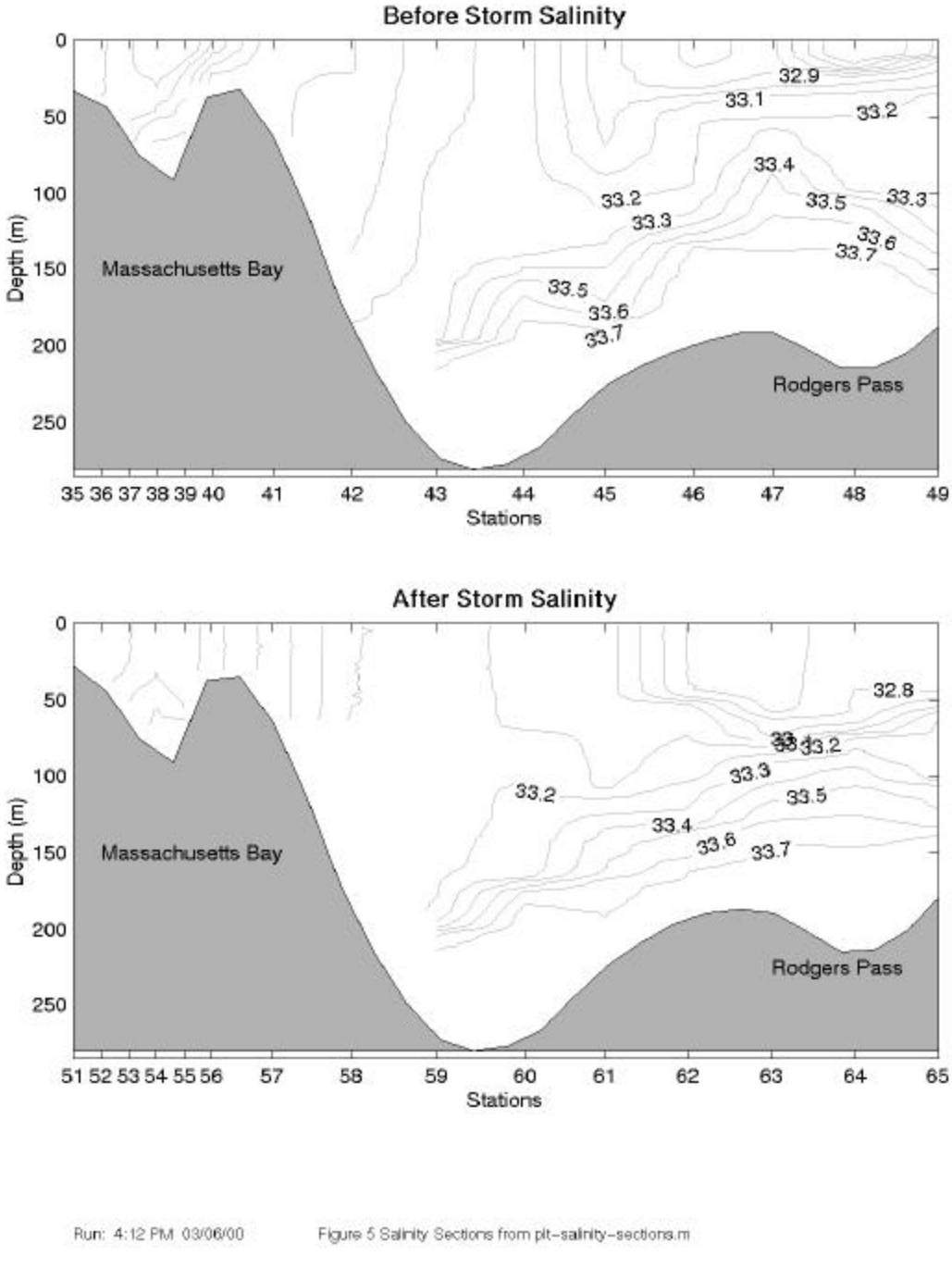

Figure 5. Salinity sections between Massachusetts Bay and Rogers Pass on 8 February 1987 just before (above) and after (below) the strong 9 February 1987 nor'easter. Note the change in location of the 33.1 isohaline relative to the Wilkinson Basin mooring on 8 February (station 44)—*before the storm*—and on 11 February (station 60)—*after the storm*.

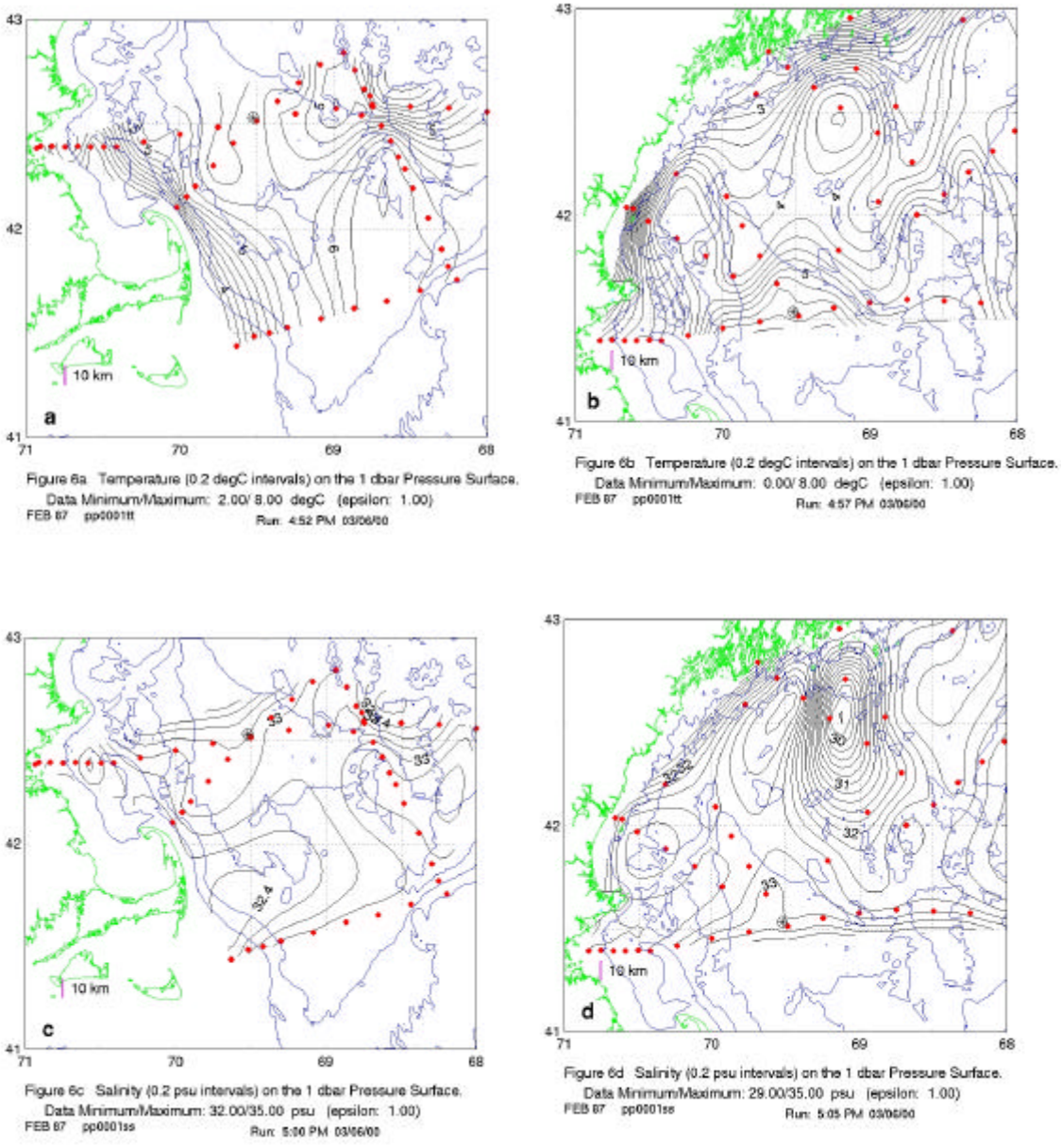

Figure 6. Surface temperature maps for (a) the pre-storm 5-8 February period and (b) the post-storm 11-20 February period (2°C contour interval). The corresponding pre-storm (c) and post-storm (d) salinity maps (0.2 psu contour interval) are shown. The hydrographic station locations are indicated.

Sea Bird temperature and conductivity sensors were used to measure temperatures at 1 m and temperatures and conductivities (T/C) at depths of 15 m, 65 m, 115 m, 165 m, respectively. Depth-time contour plots of the moored Brunt-Vaisala frequency—a measure of the water column static stability—and temperature and salinity (Figure 7) details the change of the mixed layer depth from about 120 m before the storm to about 25 m after the storm. The surface cooling was relatively strong throughout the study period. This strong temperature-induced surface buoyancy extraction by the atmosphere caused episodes of static instability of the

near-surface layer and by implication temperature-induced convective mixing events within the mixed layer. The strong cooling, associated with moderate wind stress, was sufficient to maintain the mixed layer depth at about 120 m despite the brief appearance of a fresh water anomaly on 6 February. Interestingly, some of the strongest episodes of temperature-induced instability in the upper water column occurred during the 6-9 February lull in the strong surface cooling before the storm (see Figure 7) and after this freshening event. Close inspection of this scenario (Figure 8) shows that the density instabilities coincided with this period of weak cooling interleaved between periods of daily surface warming.

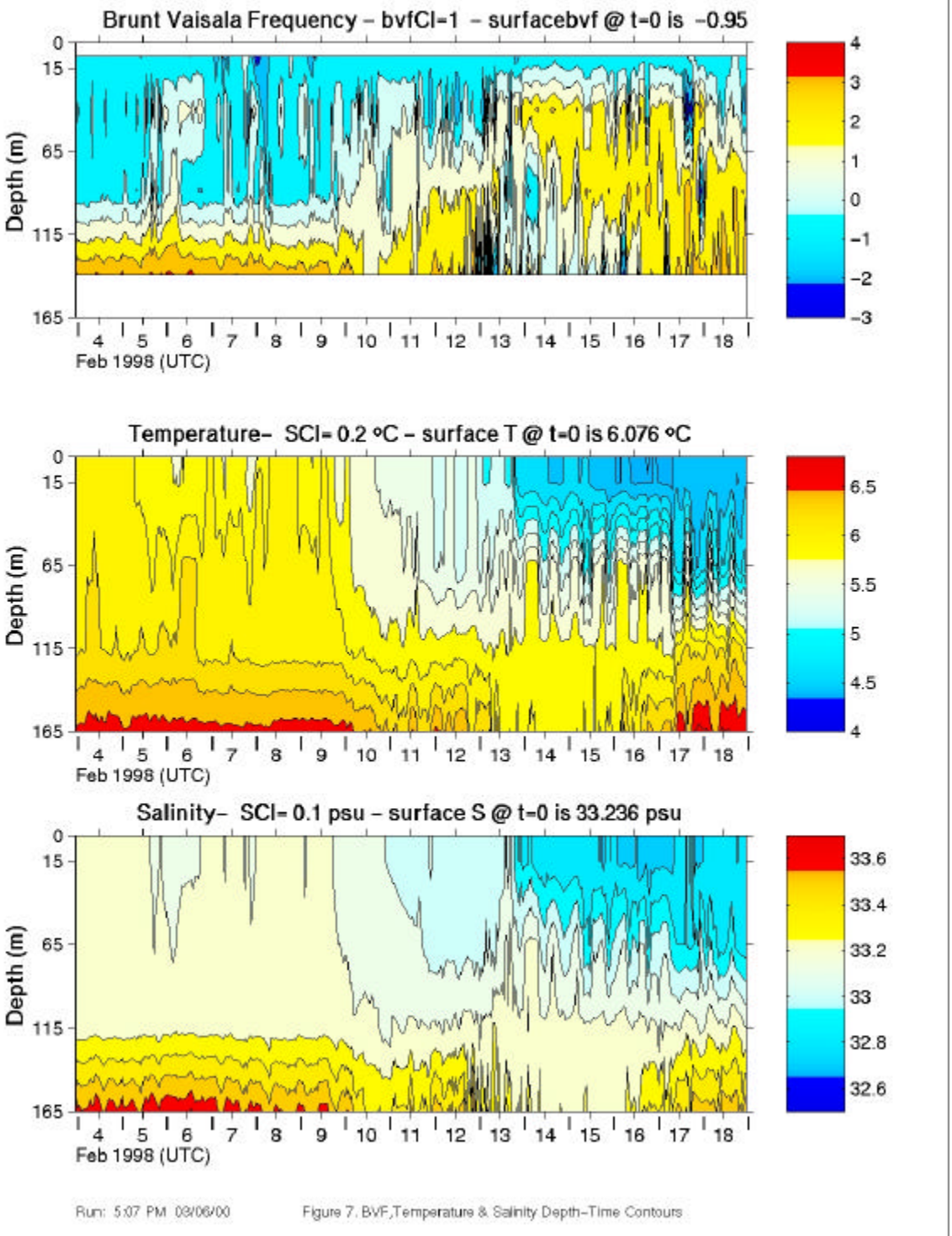

Figure 7. Depth-time contour presentations of the moored time series Brunt-Vaisala (BV) frequency, temperature (T) and salinity (S) records for 4-18 February 1987. The hourly-averaged temperature/conductivity measurements were made at the indicated depths along the abscissa. The surface values at the beginning of the records and contour intervals for BV frequency, T and S are -0.95 cph/1 cph, 6.076^{o}C/0.2^{o}C and 33.236 psu/0.1 psu, respectively.

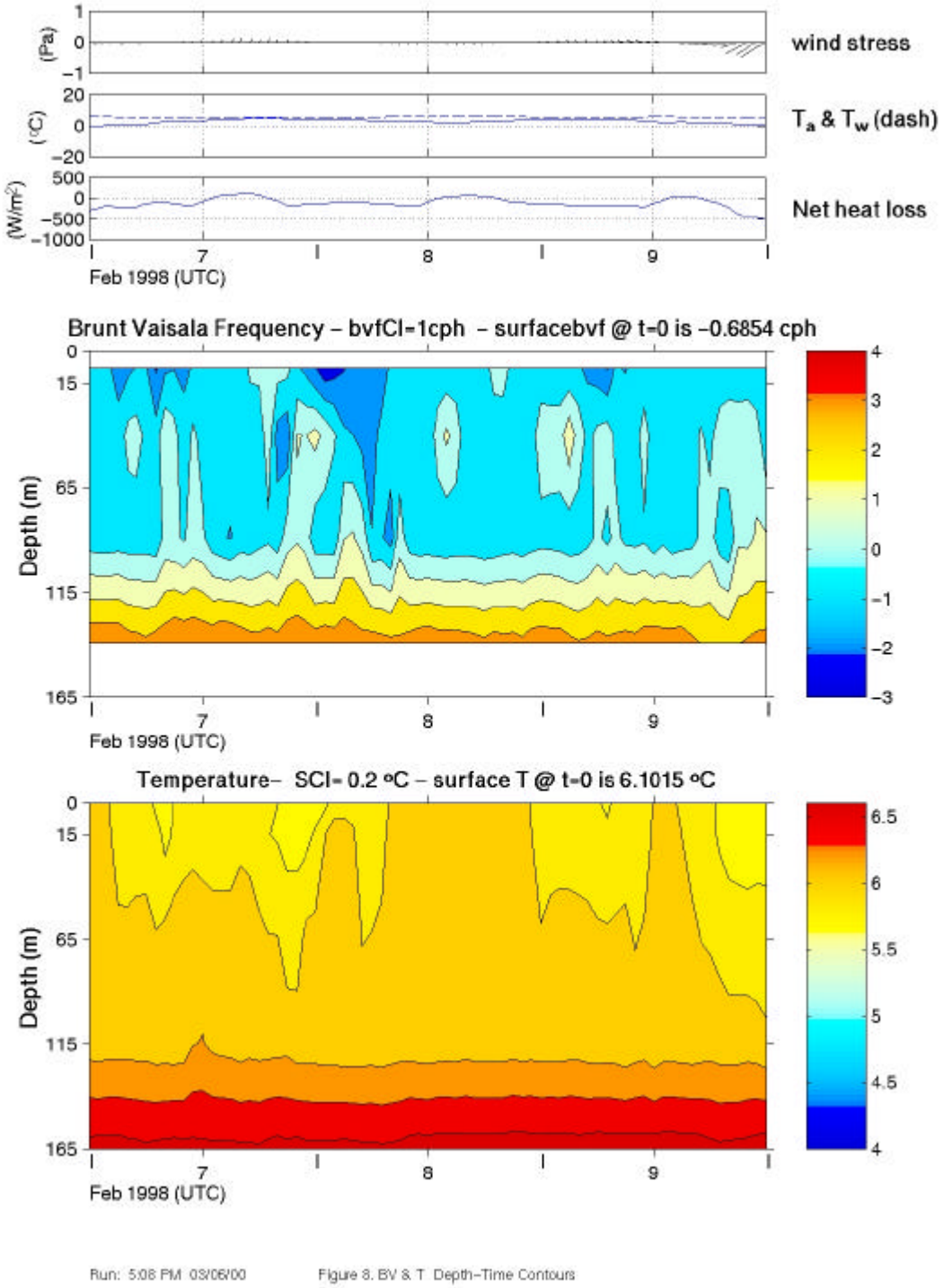

Figure 8. Pre-storm surface-cooling-induced static instability in the upper water column as revealed by depth-time presentations of Brunt-Vaisala frequency (BVF) and temperature (T). The surface values at the start and contour intervals for BVF and T are -0.68/1 cph and 6.101/0.2°C, respectively. Time series of surface wind stress, air (T_a) and sea (T_w, dash) temperatures and net surface heat flux to the ocean appear in the upper trio of panels.

The onset of the 9 February storm began a several-day period of the most intense local surface ocean cooling of the study period. The cooling was caused by a combination of strong winds and only modest air-sea temperature differences (Figure 7). Clearly storm wind-forced mechanical mixing was relatively more important than it had been during the 4-6 February cooling period. We will return to this point later in the mixed layer modeling section.

The intense cooling of 13-15 February (Figure 9), which was due to a combination of the largest air-sea temperature differences of the study period and moderate speed southeastward winds off the land, was very efficient in cooling the thinner, fresher mixed layer. There continued to be episodes of temperature-induced static instability in the upper water column—some spanning depths from the surface to about 100 m (see Figure 9)—during this period. The implied convective mixing during this period was confined to an increasingly shallower mixed layer (Figure 7). As shown in Figure 9, there were strong, unstable near-surface water patches—perhaps phase-locked to the net heat flux variability—that at times penetrated through an even shallower mixed layer.

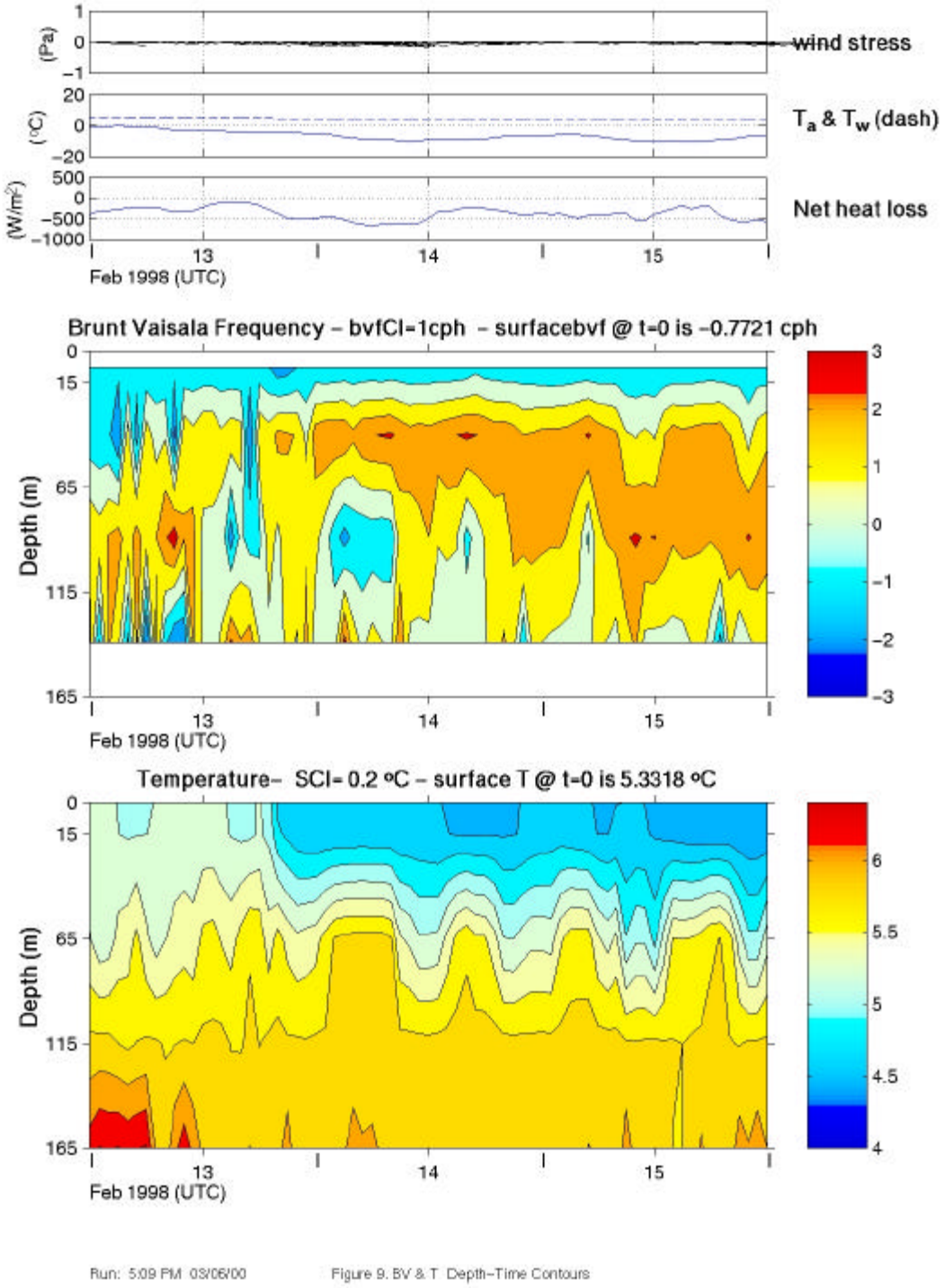

Figure 9. Post-storm surface-cooling static instability in the upper water column as revealed by the depth-time presentations of Brunt-Vaisala frequency (BVF) and temperature (T). The surface values at the start and the contour intervals for BVF and T are -0.771/1 cph and 5.332/0.2°C, respectively. Time series of surface wind stress, air (T_a) and sea (T_w, dash) temperatures and net surface heat flux to the ocean appear in the upper trio of panels.

There also was a zone of deeper mixing at this time. This is particularly evident in the water property presentations between 115 m and 165 m during 13-15 February (Figure 9). A homogeneous water mass appeared at the same place and time as a series of strong statically unstable zones (as indicated in the Brunt-Vaisala frequency) which were phased-locked with the semidiurnal tide. Thus there is a strong suggestion that the internal tide-related mixing may be a factor in the formation of winter water at depths well below the surface mixed layer.

Winter water formation is clearly indicated by the measurements. How local is the water mass formation? How well did the estimated air-sea heat extraction explain changes in the heat content changes in the Wilkinson Basin water column? To answer these questions, the net amount of heat extracted from the ocean across the sea surface (relative to the beginning of the study period) was determined (see Figure 10) by time-integrating our air-sea thermal forcing (Figure 3 and Appendix A). The heat loss (relative to the beginning of the study period) from the surface to 60 m and surface to 165 m water columns were computed through the appropriate space-time integrals of the measured temperature time series. The local heat budget for the upper ocean water column shows that decreases (increases) in heat content of the upper 60 m in Wilkinson Basin were consistent with local surface cooling (heating). (The modified TOGA-COARE heat loss estimates are consistent with water column heat loss in the upper 35 m.) However, in the 60-165 m (or 35-165 m) depth range, water column heat losses cannot be explained by local surface heat extraction processes.

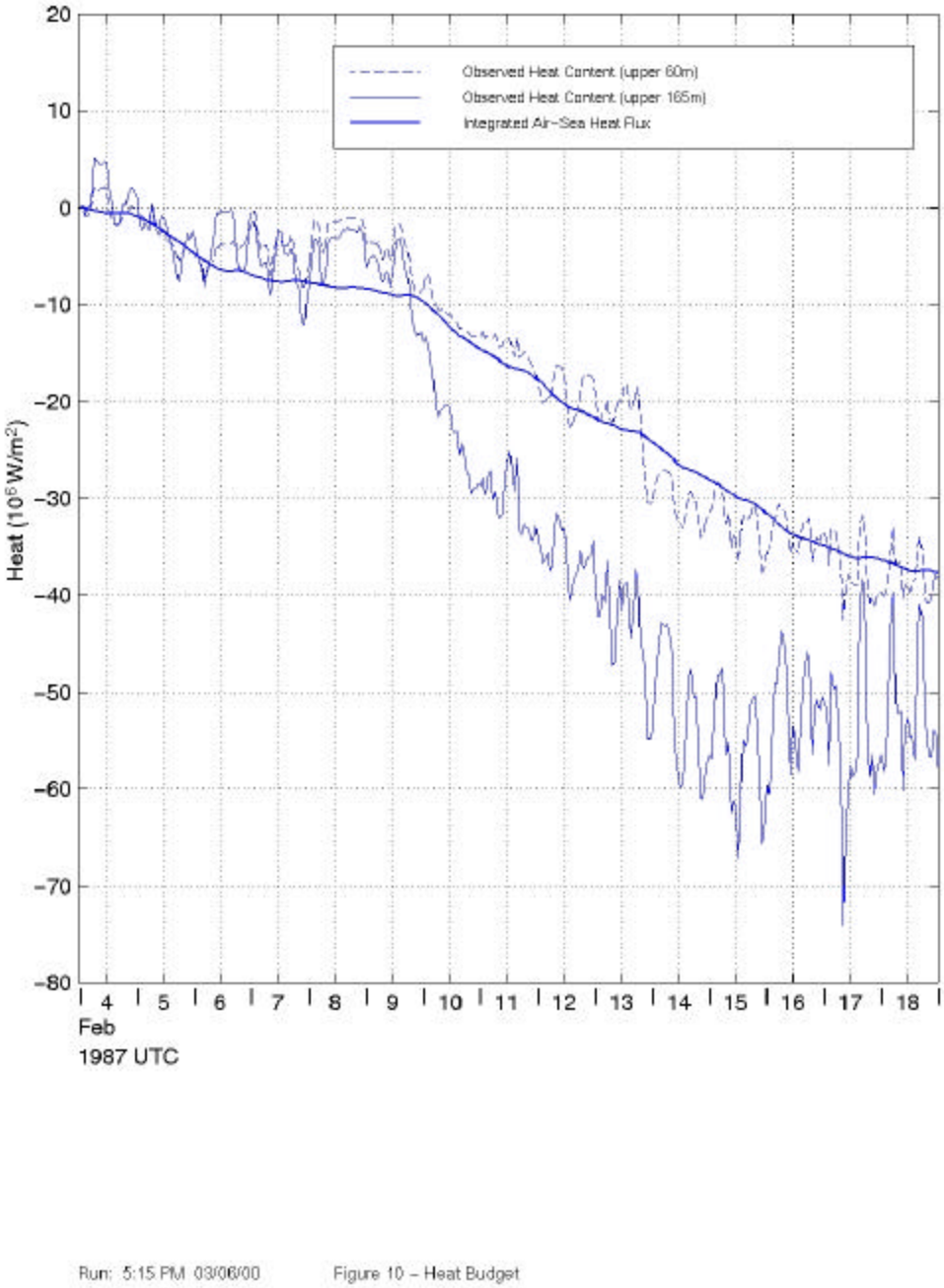

Figure 10. The computed changes in heat content in the upper 60 m (dash) and 165 m (solid) at the Wilkinson Basin buoy is compared with the time integrated net air-sea heat flux (heavy solid) (Figure 3).

The discrepancy between the local air-sea heat extraction and 165 m water column heat content change becomes most obvious after the onset of the 9-10 February storm. Inspection of Figures 7 and 9 shows the temporary 13-16 February disappearance of the "warmer" deep (100-165 m) water and the appearance of a colder 5.8^{o}C thermostad. We speculate on he origin of the colder (and fresher) water mass later.

In summary, the correspondence between the heat loss in the upper 35-60 m and the estimated local air-sea heat extraction suggests the importance of the latter at our mooring site in Wilkinson Basin. However, the fact that the deeper 100 m cools much more than can be explained by local surface heat extraction highlights the importance of the lateral advection. The apparent paradox of how advection can be important for the heat budget of the 60-165 m water column, but apparently not important for the upper 35-60 m of the water column, will also be addressed later.

Before returning to these issues, however, we present the results of two model studies of the February 1987 Wilkinson Basin. In one study, the observed momentum and heat fluxes were used to force a 1-D mixed layer model, and in the other a 3-D circulation model was employed to address issues of lateral advection during the study period. The moored observations were used to assess the performance of the 1-D model.

The Mixed Layer Model

A one-dimensional mixed layer model was used to help understand the relative effects of convective overturning and direct wind mixing in the evolution of the winter mixed layer in the Wilkinson Basin. Because of its relative simplicity and reasonable performance in previous applications, we chose the Price, Weller and Pinkel [*Price et al.,* 1986] model (henceforth PWP model) for this study. The one-dimensional PWP mixed layer formation model is driven by local surface heat and momentum fluxes and constrained by a trio of stability criteria. At each timestep, the model first checks and then mixes to ensure mixed layer static stability, followed by mixed layer dynamic stability in terms of a bulk Richardson number and finally transition layer stability.

In the PWP model, heat flux is presumed to leave directly from the sea surface, while the solar insolation is absorbed within the water column according to a double exponential depth dependence. At each time step, the one-dimensional PWP model numerically integrates the conservation equations for heat, salinity and momentum in the vertical direction to determine the respective flux profiles. Density is calculated using a linear equation of state. For this application, the model with 1/2 m vertical resolution was initialized with selected Wilkinson Basin temperature and salinity profiles and then stepped forward at one-hour increments—subject to our estimated net air-sea heat, freshwater and momentum flux forcing (Figure 3). We have diagnosed the interplay of the PWP model mixing mechanisms in terms of Wilkinson Basin conditions during a very active model mixed layer deepening episode (see Appendix B). See *Price et al.* [1986] for more detail.

The 1-D PWP [*Price et al.,* 1986] mixed layer model was applied to the Wilkinson Basin during

the three periods of strongest surface cooling, namely February 4-8 (Run 1), February 9-13 (Run 2) and February 14-18 (Run 3).

Run 1 (Figure 11): The first PWP model experiment was a 5-day run initialized with the 4 February moored hydrography, which featured a relatively deep mixed layer of about 120 m. In response to the strong cooling (due to a large air-sea temperature difference and modest winds), the *model* mixed layer depth was maintained at a relatively steady 120 m over the 2-day run. By contrast the observed mixed layer shallows briefly to about 20 m on 6 February, mixes fully on 7 February, indicates static instability early on 8 February and then mixes to 120 m later. Therefore, despite the favorable intercomparison at the end, the observed mixed layer exhibited structured changes not simulated by the model.

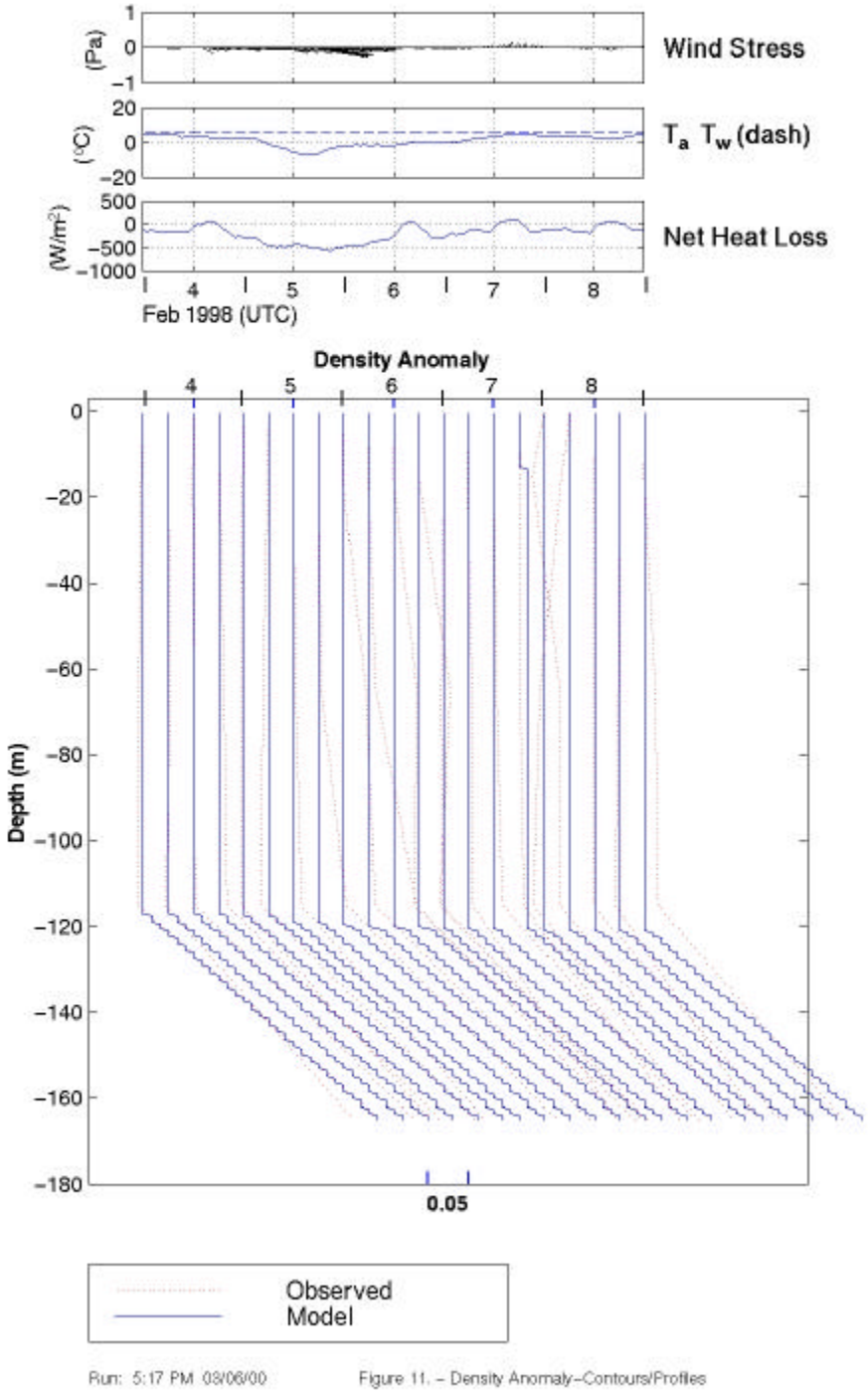

Figure 11. A 5-day sequence of 6-hourly subsamples of the hourly density PWP model anomaly profiles (solid) for 4-8 February showing how the observed initial profile (dotted) is modified by the subsequent *model* response to the *observed surface forcing* above. All profile surface densities are referenced to the appropriate date/time ticks at the top. The relative scale is given below.

Run 2 (Figure 12): The second PWP model experiment was a 3-day run initialized with 8 February hydrography. During the first day, the *model mixed layer* deepened from about 20 m to 50 m. Then during early 10 February, as the storm intensified with strong southwestward (i.e., northeasterly) wind stress and surface cooling, the *model mixed layer* deepened rapidly to about 115 m, from where it gradually decreased to 120 m during the remainder of the run.

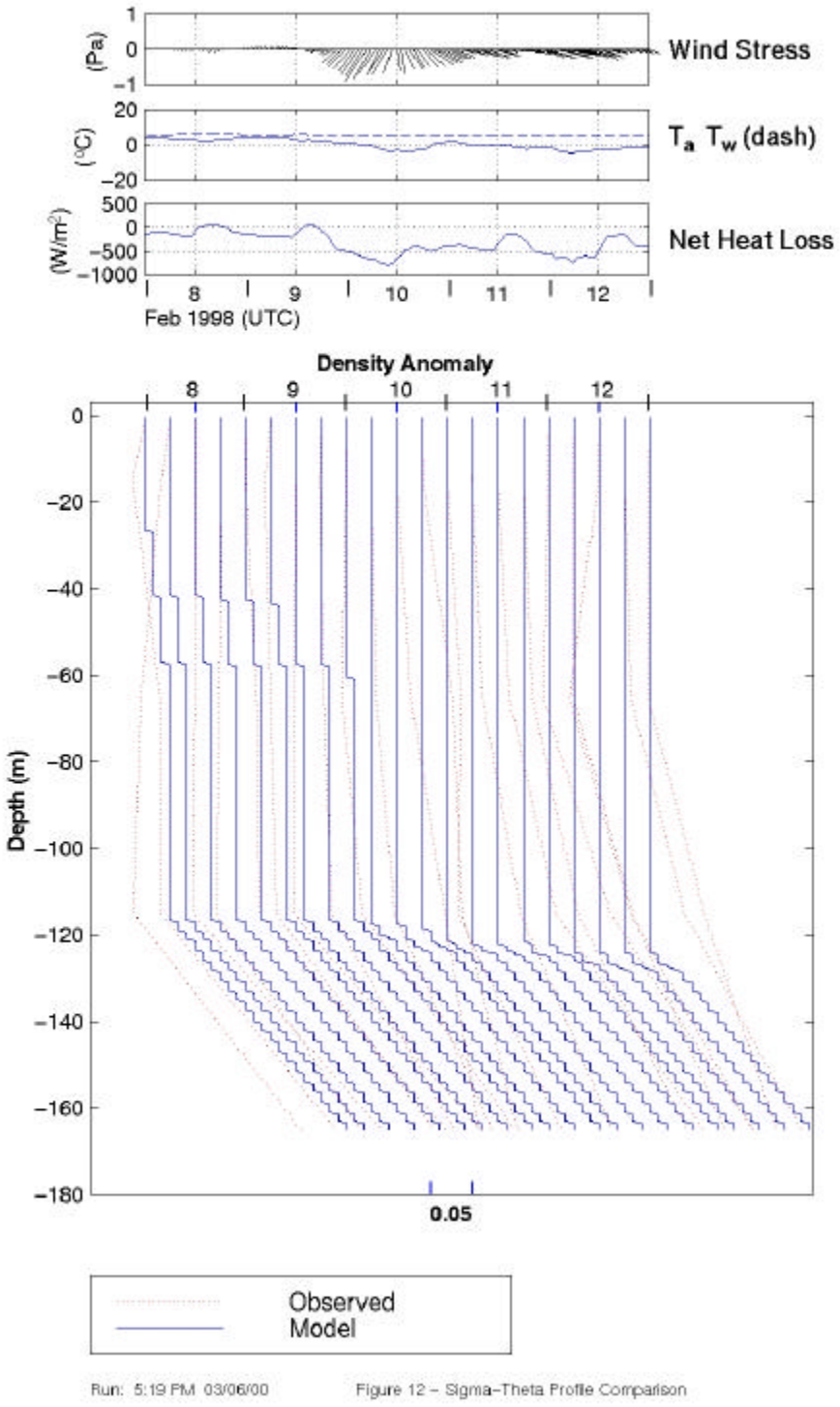

Figure 12. A 5-day sequence of 6-hourly subsamples of the hourly PWP model density anomaly profiles (solid) for 8-12 February showing how the observed moored initial profile (dotted) is modified by the subsequent model response to the observed surface forcing above. All profile surface densities are referenced to the appropriate date/time ticks at the top. The relative scale is given below.

A series of diagnostic PWP model experiments, employing different combinations of surface forcing and mixing mechanisms, were conducted for the different runs. The most instructive tests were those for run 2, which exhibited a dramatic deepening of the model mixed layer. Results of the model, with all forcings and model mixing processes active, are compared with model runs with one or more processes inactivated (Figure 13). For the test, in which only wind stress forcing and all mixing criteria were employed, the mixed layer depth equilibrated at about 80 m. For the test, in which only the net surface heat flux (and all mixing criteria) was employed, the mixed layer depth equilibrated at the full model mixed layer depth of about 120 m. The results of the latter test suggests that the convective mixing is critically important to achieving the observed mixed layer depth of about 120 m.

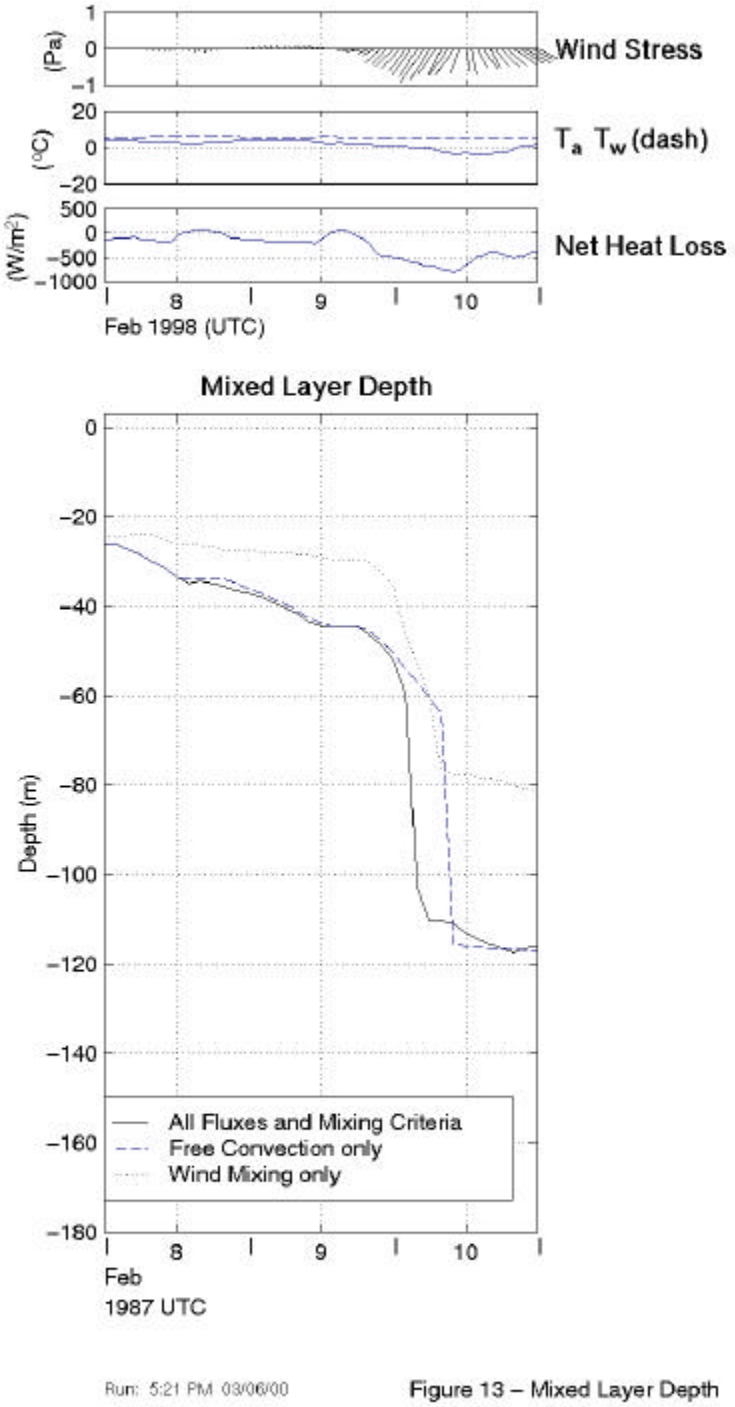

Figure 13 – Mixed Layer Depth

Figure 13. The Price, Weller and Pinkel [*Price et al*., 1987] model mixed layer depth time series for various forcing scenarios of heat fluxes and wind stresses for 8-10 February 1987. Note that (1) *model wind mixing alone* produces a maximum mixed layer depth of about 80 m and (2) *model convection mixing alone* produces a maximum mixed layer depth of about 120 m.

Run 3 (Figure 14): The third PWP model run was initialized with the 14 February hydrography which featured the salinity-induced 20 m mixed layer depth. The strong surface heat flux forcing, in the presence of modest winds, produced a gradual convection-induced deepening of the model mixed layer to a depth of 60 m. The latter was somewhat deeper than the time-averaged observed surface mixed layer depth, which was affected to a certain extent by a decreasing salinity. A series of diagnostic tests shows that convective mixing was again critically much more important than wind mixing in determining the depth of the mixed layer.

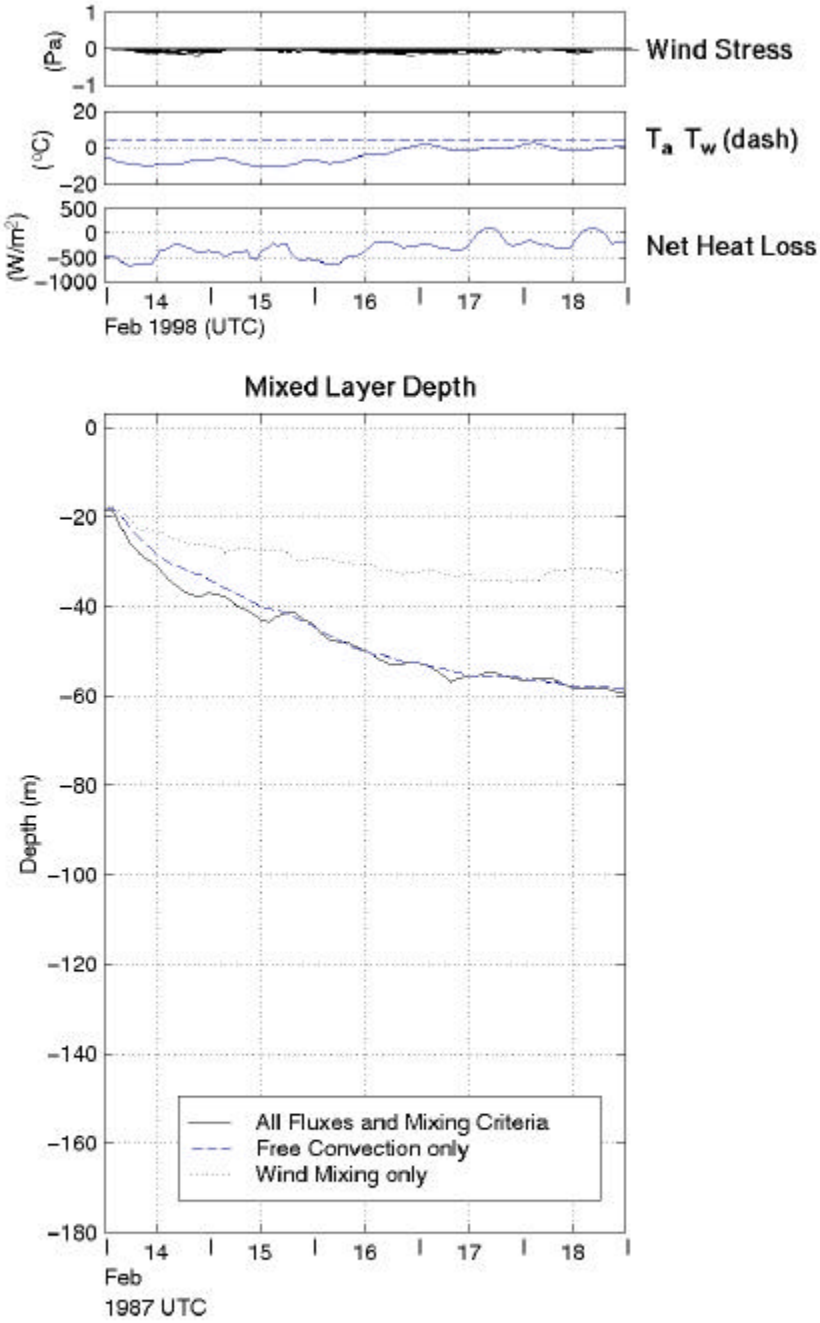

Figure 13 – Mixed Layer Depth

Figure 14. A 5-day sequence of 6-hourly subsamples of the hourly density PWP model anomaly profiles (solid) for 14-18 February showing how the observed initial profile (dotted) is modified by the subsequent *model* response to the *observed surface forcing*. All profile surface densities are referenced to the appropriate date/time tides at the top. The relative scale is given below.

So how well did the 1-D PWP model simulate the mixed layer evolution in the Wilkinson February 1987? The results were mixed. On one hand, the 5-6 February the *observed mixed layer* evolution, with some significant exceptions, was very similar to that of the model mixed layer. With the onset of the storm on 9 February, the *model mixed layer* deepened rapidly from about 20 m (after 7-8 February surface warming) to about 120 m into the near-neutrally stable deeper water. The model mixed layer depth remained at that 120 m as the surface cooling and wind stress remained strong. By contrast at the same time, the *observed mixed layer* was shallowing, first to about 60 m and then within a few days to about 25 m, due to decreasing near-surface salinity. Still, many of the 1-D PWP model/observation differences can be explained in terms of the lateral advection of a fresher near-surface water mass into the central Wilkinson Basin region, as suggested by the observations. To explore the lateral advection, we employed a three-dimensional circulation model as discussed next.

Circulation Modeling

Here we describe how observed salinity distributions are combined with horizontal velocity estimates from the Dartmouth linear, harmonic finite-element circulation model of the Gulf called FUNDY [*Lynch and Naimie*, 1993] to help explain differences between PWP model and observational results. The constant density, 21-level model was run in the near steady-state (i.e., very low frequency) to simulate the wind-driven 3-D current field on a domain including the Gulf and adjacent regions (Figure 15) for each day of the study period. The circulation model was forced with 36-hour-average, spatially variable wind stress fields derived using the optimal spatial interpolation scheme, as described by *Feng and Brown* [1998], and NDBC wind measurements. Halifax sea level was used to simulate remote wind forced effects along the backward cross-shelf boundary. The open ocean boundary sea level was clamped to zero, while geostrophic flow was allowed to leave the westernmost across-shelf boundary.

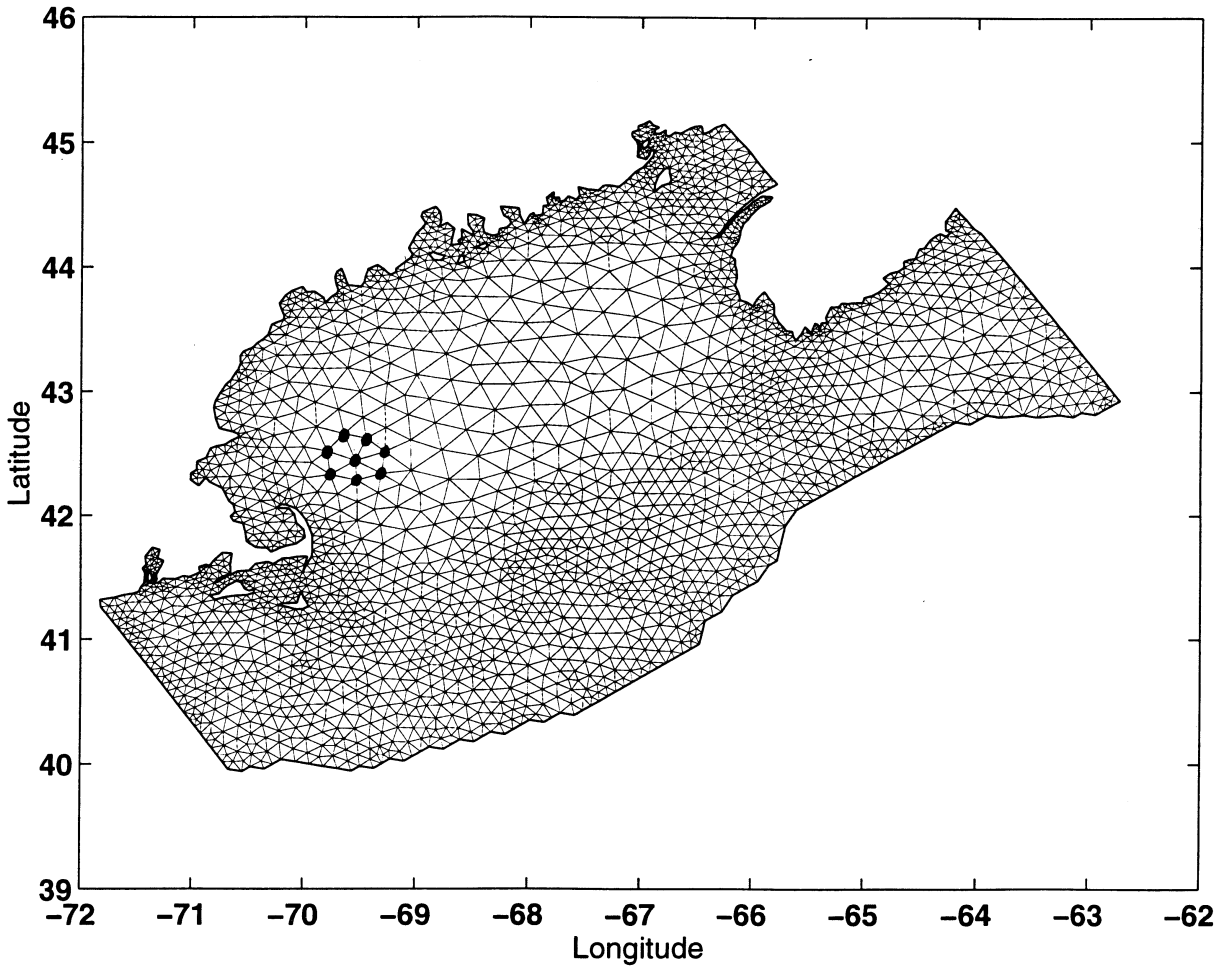

Figure 15. The "gbl" finite element mesh used for the FUNDY 5 circulation model of the horizontal current field at 8 sites in Wilkinson Basin.

The current profiles at 8 model mesh nodes in the Wilkinson Basin (Figure 15) for the first day of the storm (9 February 1987) show a distinct near-surface Ekman layer flow above the slower and near depth-independent deeper flow (Figure 16). The model currents were vertically averaged over both the upper 45 m Ekman layer and a deep layer extending from 45 m to the bottom (about 270 m). The Figure 17a plot of these depth-averaged flows shows a strong southwestward net flow of about 15 km/day in the 45 m thick upper Ekman layer, in contrast to the much weaker generally southeastward deeper layer flow on 9 February. On the second day of the storm (February 10) the model wind-driven flow in the upper layer was still toward the southwest (Figure 17b) and even stronger than on 9 February. The 10 February picture shows that clockwise (anticyclonic) flow of about 4 km/day appears to have also developed at depth in the Wilkinson Basin (Figure 17b) and strengthened by 11 February (Figure 17c). With the

passing of the storm, the intensity of the 12 February deep flow pattern weakened (Figure 17d), with the deep wind-driven gyre all but disappearing by 14 February (not shown).

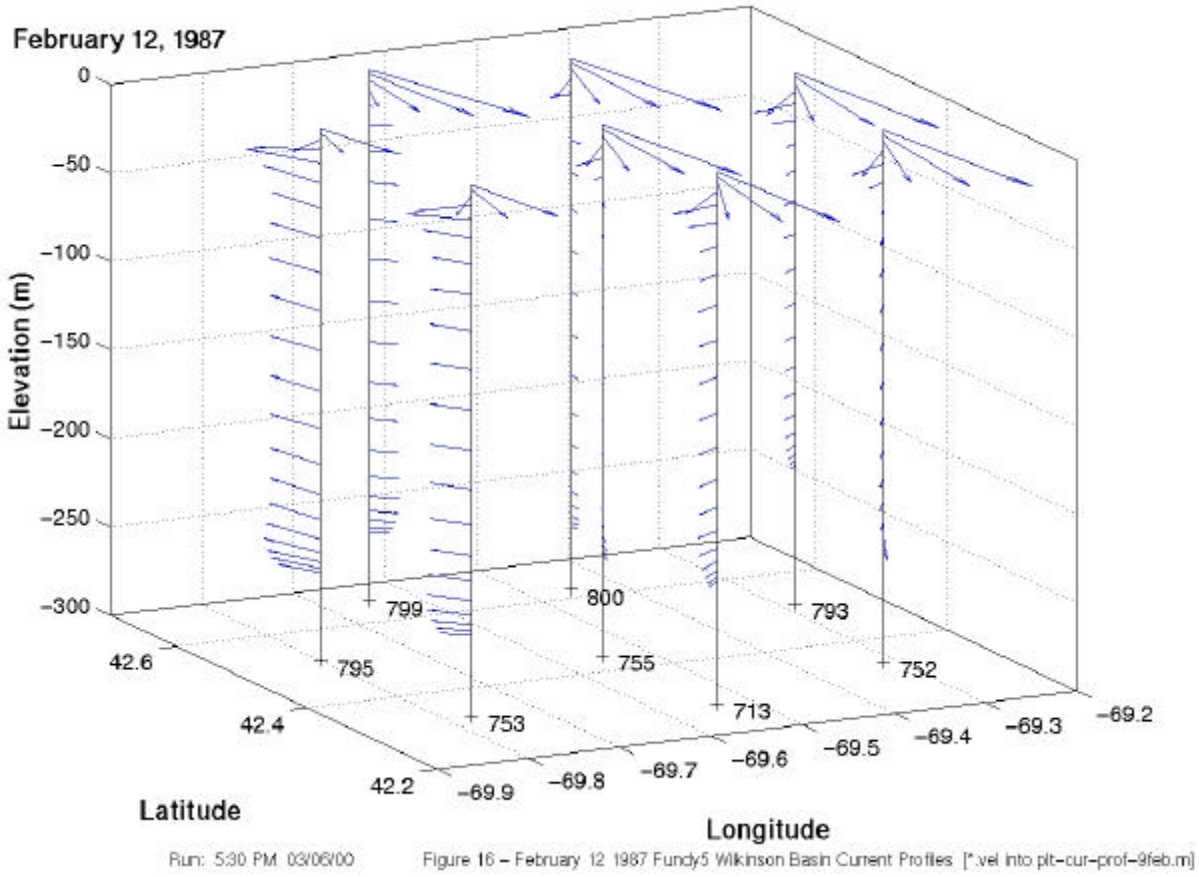

Figure 16. A perspective presentation of the FUNDY model current profiles at the 12 February 1987 Wilkinson Basin nodes located in Figure 15. Note the distinct storm wind-driven Ekman layer currents which contrast with the less intense and nearly uniform deeper currents.

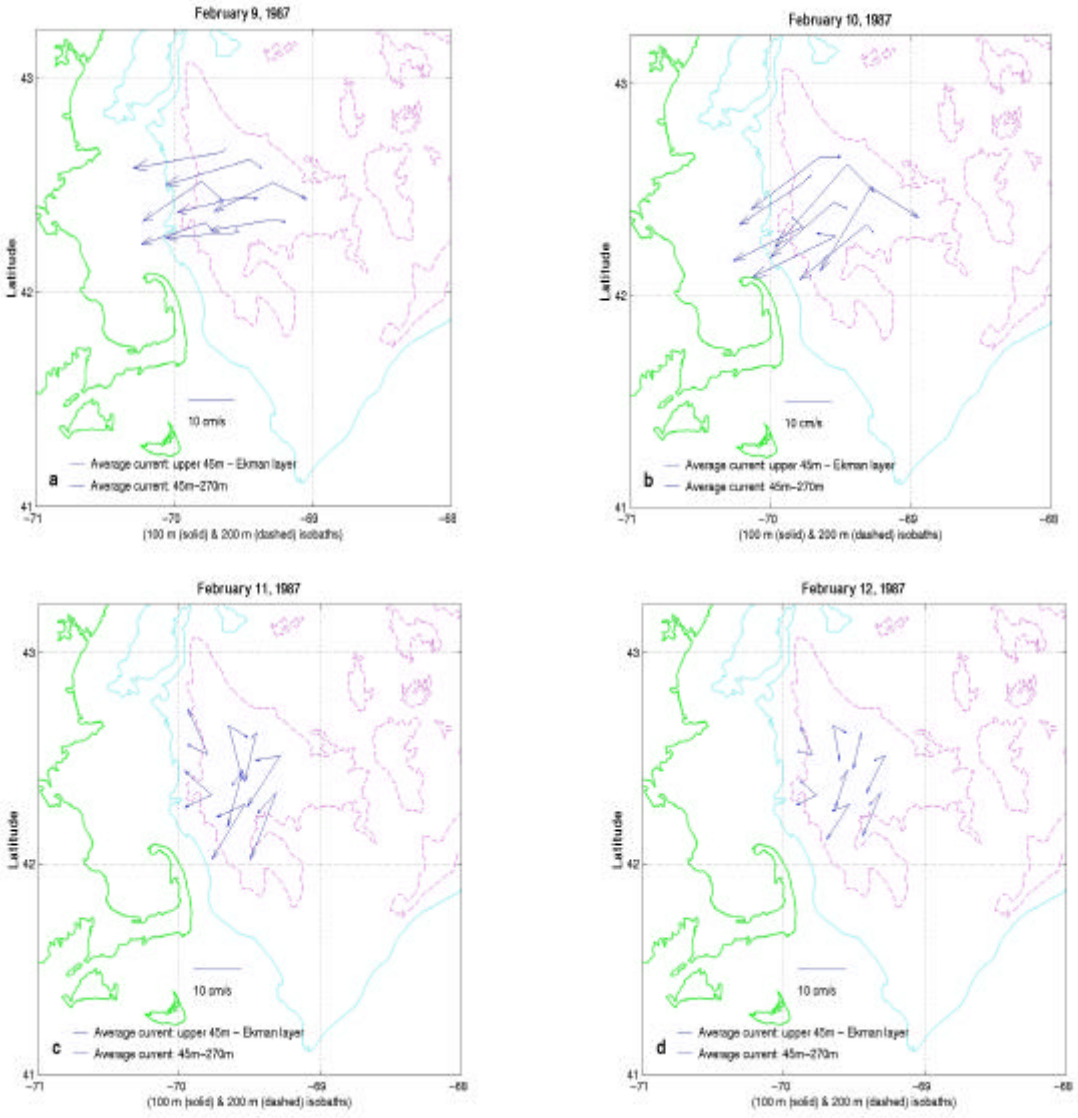

Figure 17. Vertically averaged FUNDY Ekman layer and deep currents for (a) 9 February 1987, (b) 10 February, (c) 11 February and (d) 12 February, respectively.

These model results strongly suggest the existence of a significant wind-driven shear throughout the upper 50 m of the mixed layer. Thus we conclude that any small scale convective plumes would be significantly sheared and thus become 3-dimensional. These model results also suggest that northeast storms can produce transient deep anticyclonic gyre flow—an intermittent process which probably has a role in the production of the cold, intermediate depth (100-165 m) water mass seen in the 13-16 February observations.

Discussion

The circulation model flow results suggest that there was significant lateral advection in the upper 50 m within Wilkinson Basin, particularly during the storm. The Ekman transport quite likely advected the fresher surface waters to the east and northeast of Wilkinson Basin—hinted at

in the Figure 6 surface salinity maps—toward the Wilkinson Basin mooring site. The estimated temporal change of salinity in Wilkinson Basin induced by lateral advection (the product of the observed salinity gradients and the model upper layer transports) was a decrease of 0.14 psu between 9-12 February. This advection-based result agrees very well with the salinity decrease of 0.15 psu measured at the Wilkinson Basin mooring. Thus we conclude that the observed freshwater-induced restratification of the upper water column in Wilkinson Basin during and after the storm clearly was due to the storm-forced advection of water from north and east of Wilkinson Basin toward the mooring.

With such significant lateral advection in the upper 50 m, why did the upper 50 m of the Wilkinson basin water column "seem" to be locally cooled during the study period? The answer seems rooted in the observed surface temperature fields (Figure 6a) which show relatively weak temperature gradients in northeast-southwest strips parallel to the NH-Maine coast—a pattern consistent with the effects of the cold, dry winds which move southeastward offshore. Thus it appears that the generally southwestward Ekman transport during the study period advected cooled water with similar cooling histories parallel to the coast toward Wilkinson Basin.

The origin of the cooler water appearing in the deeper Wilkinson water column is probably the coast. *Brown and Beardsley* [1978] have documented the production of very cold water in the western Gulf south of Boothbay Harbor. The *Brown and Irish* [1993] hydrographic observations document the same for Jeffreys Basin and Bank region and Massachusetts Bay. Thus we hypothesize that cold, dense coastal water most likely *descended* from these regions into the region of Wilkinson Basin and was entrained by the deep, wind-forced gyre there during the study period.

Seeking evidence regarding that hypothesis, we mapped the shape of the 26.2 Φ_2 surface for the post-storm period under study (Figure 18). Clearly that surface, which intersects the Wilkinson Basin mooring site at a depth of about 160 m, shallows to the bottom depths of coastal regions near 44.0^{o}N, 69.3^{o}W (south of Boothbay Harbor) and in and around Jeffreys Bank and Basin (43^{o}N, 70.2^{o}W). Temperature and salinity distributions on the 26.2 Φ_2 density surface show that the coastal water, which could "slide" from the coastal regions via gravity-like currents, would start out with properties of about 4.2^{o}C and 33 psu. These properties would evolve in transit, presumably through 3-D mixing processes, to Wilkinson Basin water of 6.3^{o}C and 33.2 psu. These are the properties of deep Maine Intermediate Water. The locally formed cold water may possibly be blended with the coastal water via breaking internal tidal waves and distributed laterally throughout the Wilkinson Basin by the intermittent clockwise (westward wind-forcing) and counter-clockwise (eastward wind-forcing) deep Wilkinson Basin wind-forced circulations. The latter speculations remain hypotheses to be tested.

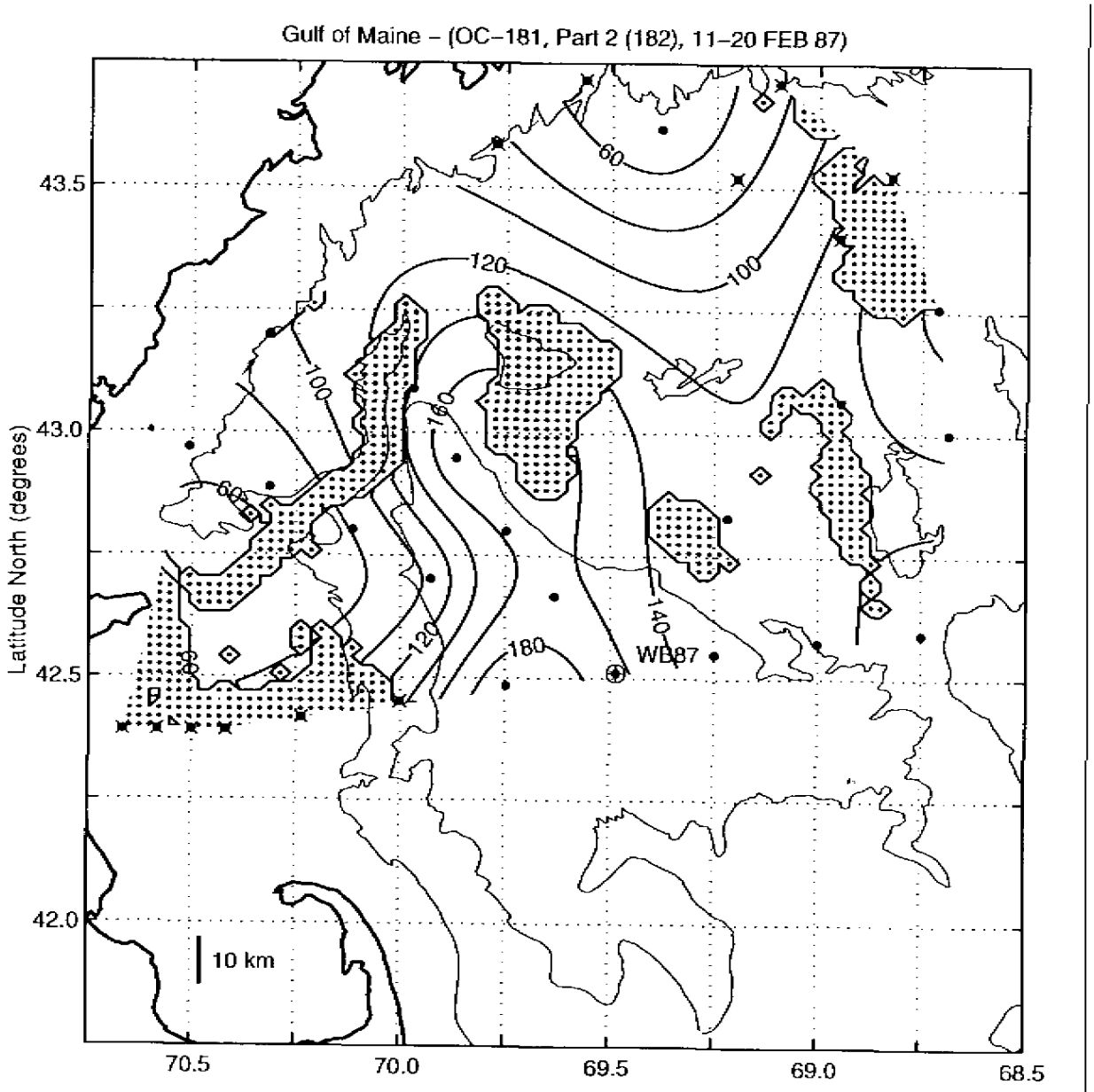

Figure 18. The post-storm depiction of the depth (m) of the 26.2 sigma-theta surface in the region north of the Wilkinson Basin mooring site. Note how this surface, which outcrops in the near coastal regions surrounding Wilkinson Basin, sinks to about 160 m in the vicinity of the mooring.

Summary of Results

(1) Two types of cooling events in February 1987. The 5-6 and 14-16 February cooling events were due to modest offshore wind stress and relatively large air-sea temperature differences. The 9-11 February storm-induced cooling event was due to high wind stress and modest air-sea temperature differences.

(2) Observed and PWP model 4-6 February 1987 mixed layers were similar. The high surface

heat loss caused convection in the near-neutrally stable water column, thus maintaining the mixed layer depth at ~120 m. The cold (and dry) offshore winds produced minimal lateral advection.

(3) Free convection was critical in the initial deepening of the 9 February 1987 Wilkinson Basin mixed layer to a depth of 120 m. Model results suggest that wind stress alone would have deepened the mixed layer to depths of only about 80 m.

(4) The 9-10 February 1987 storm-forced lateral advection of surface layer fresher water from the northeast increased the local static stability of the water column and shallowed the near surface mixed layer.

(5) The convective circulations in the upper layer of the Wilkinson Basin mooring site must be very 3-dimensional, due to the presence of sheared wind-forced Ekman flow.

(6) The deeper water column in Wilkinson Basin appears to have been fed by colder, denser water formed in adjacent coastal regions in the western Gulf.

Appendix A: Heat Flux Estimates

The average solar insolation for the 8-18 February 1987 was derived from the *Hopkins and Garfield* [1979] climatological monthly regression for February

$$Q_I(\text{gm-cal/cm}^2\text{/s}) = (1.73\ s + 90.08)/3600 \quad ,$$

where *s* is the percent of total possible hours of sunshine. The average of total number of hours of sunshine for Portland, Maine, 8-18 February 1987, is 10.2 hours according to the Astronomical Applications Department, U.S. Naval Observatory. The diurnal variation of the solar insolation was simulated by a sinusoid with amplitude Q_I according to

$$Q_I(t) = [\mathrm{B} Q_I/(2T_d)] \times \sin[\mathrm{B}\ (t - T_{sr})/T_d] \quad ,$$

when

$$T_{sr} < t < (T_d + T_{sr})$$

and when

$$T_{sr} > t > (T_{d=+}\, T_{sr}), \quad Q_I\,(t) = 0 \quad ,$$

where

t is the time in hours since midnight of each day. T_d is the total number of hours of sunshine and T_{sr} is the time of sunrise for each day (from time of sunrise and sunset observations at Portland, Maine, by the U.S. Naval Observatory).

The long wave (IR) back radiation (Q_b, W m^{-2}) was computed according to the relation [*Berliand and Berliand*, 1952]:

$$Q_b = 1.1365 \times 10^{-7}\ (t_w + 273.15)^4\ (0.39 - 0.05e_a)\ (1 - 0.0068c^2) \times 0.484 \quad ,$$

where t_w is the sea surface temperature (^{o}C) (by the UNH WB mooring surface at 1 m) and *c* is the % cloud cover (assumed to be a constant 50% for the entire period), and e_a is the water vapor pressure (mb) of air at anemometer height (10 m) (see below).

The latent heat flux was computed according to the relation [*Brown and Beardsley*, 1978]

$$Q_e = E\ L \quad ,$$

where the coefficient of latent heat *L* is

$$L\ (\text{cal/gm}) = 596 - 0.52\ t$$

and the evaporative mass flux E is

$$E\ (\mathrm{gm/cm^2/day}) = 0.007\ (EW - e_a)\ W \quad ,$$

where W is the wind speed (knots) and the water vapor pressures at the sea surface e_w and at anemometer height e_a are determined as follows. The water vapor pressure at the sea surface temperature e_w is

$$e_w(\mathrm{mb}) = e_{sd}\ (1 - 5.37 \times 10^{-4}\ S) \quad ,$$

where S is salinity (assumed to be 33 psu), and e_{sd} is the saturated water vapor pressure of distilled water at sea water temperature t_w evaluated according to [*Dutton*, 1986]:

$$e_{sd} = 6.11 \exp\left[(L/0.1104)\ (t_a/273.16\ (t_a + 273.16))\right] \quad ,$$

where t_a is the air temperature (^{o}C) at anemometer height. The water vapor pressure at anemometer height is determined from relative humidity according to

$$e_a = RH\ e_{sd} \quad ,$$

where RH is the relative humidity at anemometer height (assumed to be a constant 77% for the entire 11-day period). We have assumed that sensible heat flux Q_h is related to latent heat flux according to

$$Q_h = BQ_e \quad ,$$

where B is the Bowen ratio [*Bowen*, 1926] given as

$$B = 0.49\ (t_w - t_a)\ /\ (e_w - e_a) \quad .$$

Appendix B: PWP Model Mechanics

Here we diagnose the mechanics of the PWP model for the particularly dramatic storm-related model mixed layer deepening event of 9-10 February 1987. At each of the hourly model time steps (see Figure 20 details), the model temperature profile is modified as the results of four considerations, namely

(1) *Heat is extracted* from (added to) the upper model grid according to the surface forcing during the previous time step;

(2) *Static instability* is eliminated through convection and entrainment of water at the base of the mixed layer and homogenization;

(3) *Mixed layer-scale dynamic instability*, due to both stratification strength and shear induced by wind stress forcing (see 2nd panel above) and measured by a bulk Richardson number Rb (see below), is eliminated through entrainment at the base of the mixed layer and homogenization

$$R_b = (g\ )\ \Delta h / \Delta_0\ (\ )\ \mathbf{V})^2)\quad 0.65\quad ,$$

where *h* is the mixed layer depth and)**V** and)Δ represent the differences in the values of velocity **V** and Δ in the mixed layer and the level just below;

(4) *Small-scale dynamic instability* at the base of the mixed layer, as measured by the gradient Richardson number Rg (see 3rd panel above), is eliminated through small scale mixing (i.e., smoothing) in the transition layer, where

$$R_g = (g\ (M\Delta / Mz) / \Delta_0\ (M\mathbf{V} / Mz)^2) \exists\ 0.25\quad .$$

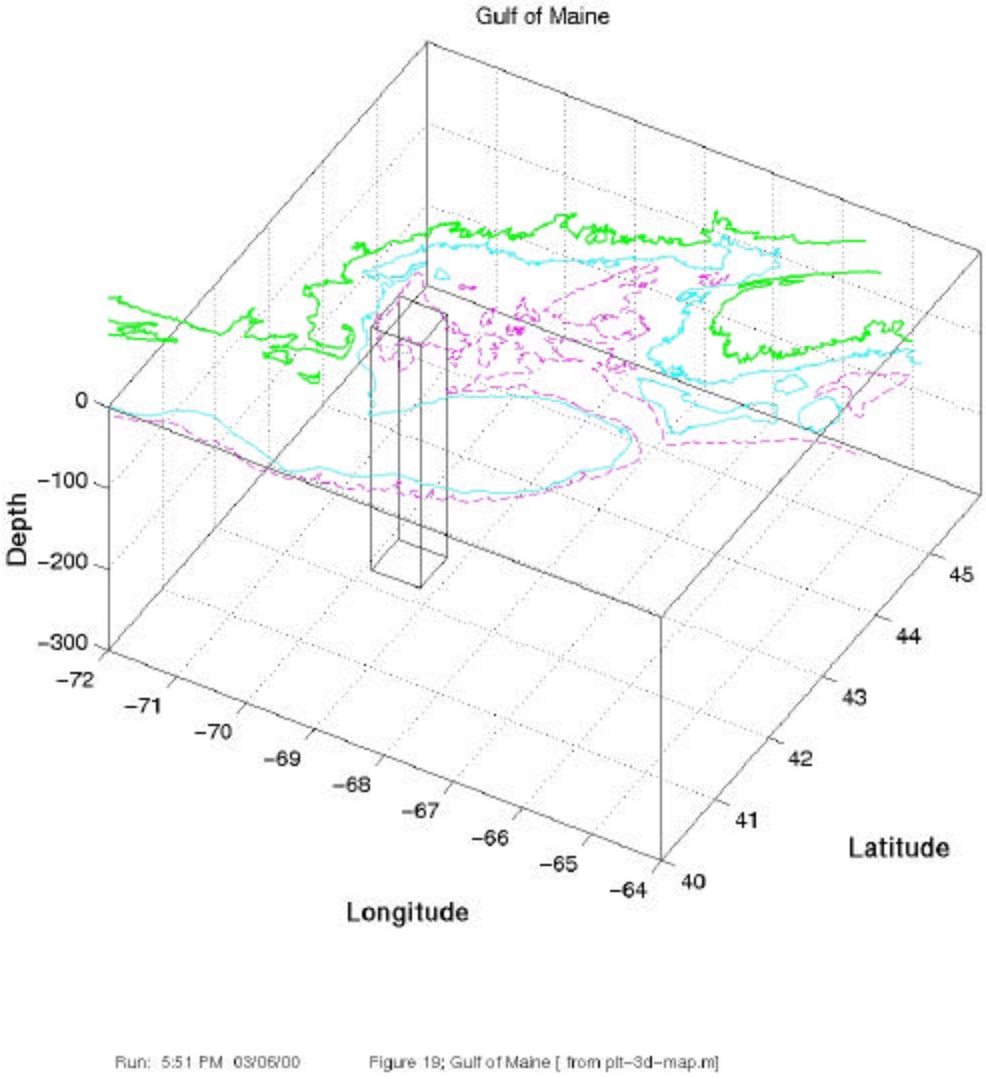

Figure 19. A schematic of the hypothesized sinking and flow of dense coastal water to the region of the deep Wilkinson Basin anticyclone.

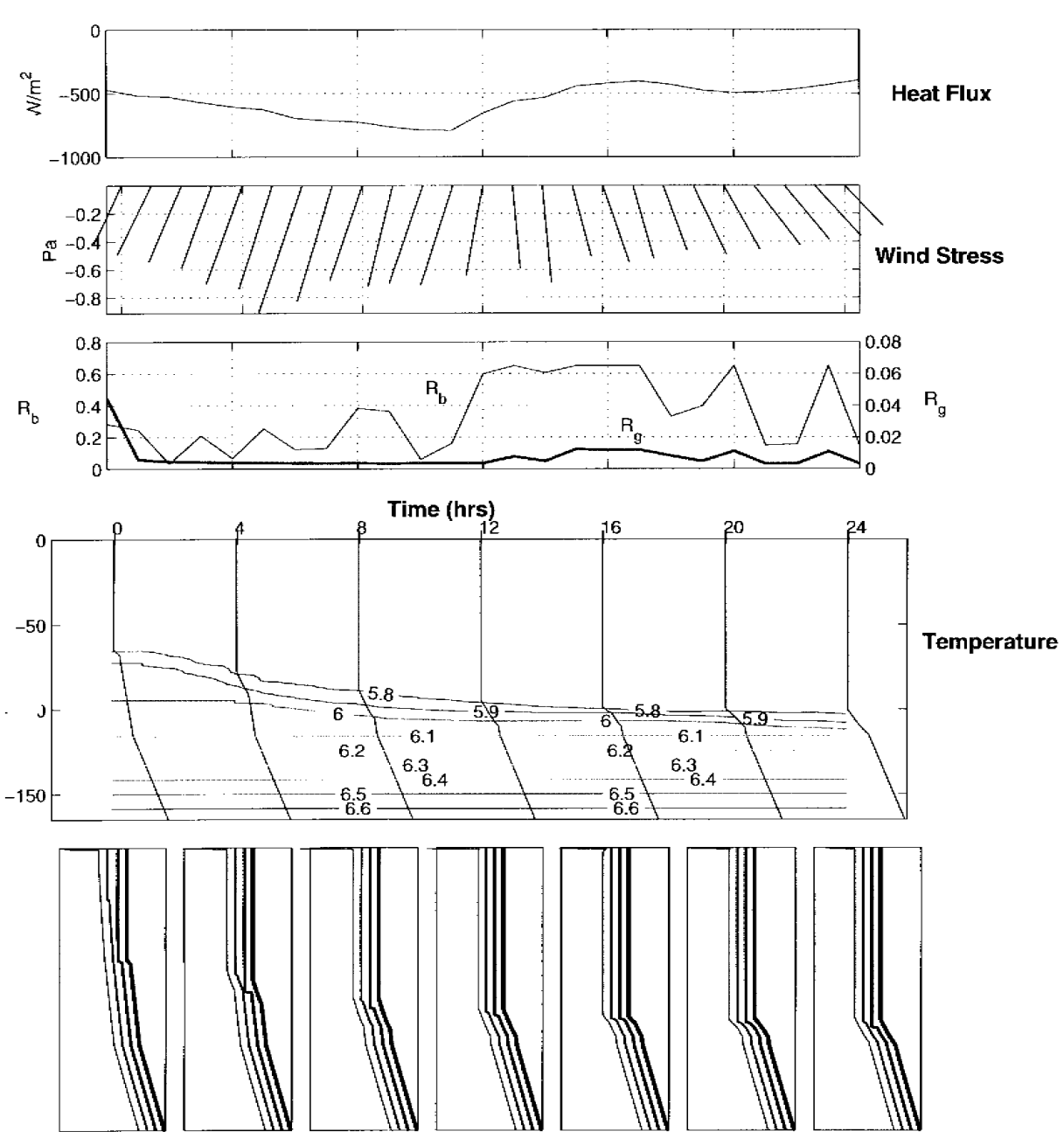

Figure 20. A case study of the PWP mechanisms responsible for producing the dramatic *model* mixed layer deepening in response to the 10 February 1987 surface heat flux and wind stress forcing (top two panels). The model temperature profiles with corresponding isotherms are shown for every *fourth* model time step in the middle panel. The bottom panel shows the sequence of model temperature profiles—modifications each time step—starting with the effects of surface forcing (left) and progressing through the three mixing mechanisms to the "final" profile (right). The time series of bulk and gradient Richardson numbers are shown in the third panel.

This process maintains a smooth transition layer at the base of the mixed layer.

Acknowledgments. This research has benefitted from the contributions of many people,

including J. Price, who made the mixed layer model available to us, D. Lynch and his coworkers, who have helped us learn to use the Dartmouth models wisely, Frank Bub and Don Denbo, with whom we have had stimulating discussions on this topic. Support for PM and WSB was provided by the National Science Foundation under grant OCE-9530249.

References

Berliand, M.E., and T.G. Berliand, 1952. Determination of effective radiation of the earth as influenced by cloud cover, *Izv. Akad. Nauk S.S.S.R. Ser. Geogr. Geofiz., 1*, 64-78.

Beardsley, R.C., E.P. Dever, S.J. Lentz, and J.P. Dean, 1998. Surface heat flux variability over the northern California shelf, *J. Geophys. Res., 103*, 21,553-21,586.

Bowen, I.S., 1926. The ratio of heat losses by conduction and evaporation from any water surface, *Phys. Rev., 27*(6), 779-787.

Brown, W.S., and R.C. Beardsley, 1978. Winter circulation in the Western Gulf of Maine: Part 1. Cooling and water mass formation, *J. Phys. Oceanogr., 8*, 265-277.

Brown, W.S., and J.D. Irish, 1993. The annual variation of water mass structure in the Gulf of Maine: 1986-1987, *J. Mar. Res., 51*, 53-107.

Bunker, A.F., 1956. Measurements of counter gradient heat flows in the atmosphere, *Aust. J. Phys., 9*, 133-143.

Clarke, R.A., and J.C. Gascard, 1983. The formation of Labrador Sea Water. Part I: Large-scale processes, *J. Phys. Oceanogr., 13*, 1764-1778.

Dutton, J.A., 1986. The Ceaseless Wind: An Introduction to the Theory of Atmospheric Matron, Dove Publication Inc., NY, 617 pp.

Fairall, C., E.F. Bradley, D.P. Rogers, J.C. Edson, and G.S. Young, 1996. Bulk parameterization of air-sea fluxes for the Topical Ocean-Global Atmospheric Coupled-Ocean Atmospheric Response Experiment, *J. Geophys. Res., 101*, 3747-3764.

Feng, H., and W.S. 1999. Brown, The wind-forced response of the western Gulf of Maine coastal ocean during spring and summer 1994, submitted to *J. Geophys. Res.*

Hopkins, T.S., and N. Garfield III, 1979. Gulf of Maine Intermediate Water, *J. Mar. Res., 37*, 103-139.

Killworth, P.D., 1983. Deep convection in the world ocean, *Rev. Geophys. Space Phys., 21*, 1-26.

Large, W.S., and S. Pond, 1981. Open ocean momentum flux measurements in moderate to strong winds, *J. Phys. Oceanogr., 11*, 394-410.

Lynch D.R., and C.E. Naimie, 1993. Three-dimensional diagnostic model for baroclinic wind driven tidal circulation in shallow seas; FUNDY 5 user's manual, Lab. Rep. NML-93-1, Dartmouth College, Hanover, New Hampshire, 40 pp.

Price, J.F., Weller, R.A., and R. Pinkel, 1986. Diurnal cycling: Observations and models of the upper ocean response to diurnal heating, cooling and wind mixing, *J. Geophys. Res., 91*, 8411-8427.

Stommel, H., 1972. Deep winter-time convection in the western Mediterranean Sea, in: Studies in Physical Oceanography, a Tribute to George Wust on his 80th Birthday, edited by A. L. Gordon, pp. 207-208, Gordon and Breach 2.